uOttawa

L'Université canadienne
Canada's university

FACULTÉ DES ÉTUDES SUPÉRIEURES ET POSTOCTORALES

uOttawa

L'Université canadienne
Canada's university

FACULTY OF GRADUATE AND POSDOCTORAL STUDIES

Stephanie J. Silva
AUTEUR DE LA THÈSE / AUTHOR OF THESIS

M.Sc. (Neuroscience)
GRADE / DEGREE

Department of Cellular and Molecular Medicine
FACULTÉ, ÉCOLE, DÉPARTEMENT / FACULTY, SCHOOL, DEPARTMENT

Identifying the Effects of mutations in the Rab Domain on Leucine-Rich Repeat Kinase 2 (LRRK2) Function

TITRE DE LA THÈSE / TITLE OF THESIS

Johnny Ngsee
DIRECTEUR (DIRECTRICE) DE LA THÈSE / THESIS SUPERVISOR

CO-DIRECTEUR (CO-DIRECTRICE) DE LA THÈSE / THESIS CO-SUPERVISOR

EXAMINATEURS (EXAMINATRICES) DE LA THÈSE / THESIS EXAMINERS

Mario Tiberi

Kursad Turksen

Dr. Guy Drouin

Gary W. Slater
Le Doyen de la Faculté des études supérieures et postdoctorales / Dean of the Faculty of Graduate and Postdoctoral Studies

Identifying the Effects of Mutations in the Rab Domain on Leucine-Rich Repeat Kinase 2 (LRRK2) Function

Stephanie J. Silva
Supervisor: Johnny K. Ngsee

This thesis is submitted as a partial fulfillment of the M.Sc. program in Neuroscience.

Thesis submitted to the
Department of Cellular and Molecular Medicine
Faculty of Graduate and Postdoctoral Studies
University of Ottawa

Final Date of Submission: October 6, 2008
Place of submission: Faculty of Graduate and Postdoctoral Studies
University of Ottawa
75 Laurier Avenue East, Ottawa, ON

uOttawa

L'Université canadienne
Canada's university

Your file Votre référence
ISBN: 978-0-494-46499-1
Our file Notre référence
ISBN: 978-0-494-46499-1

ABSTRACT

Parkinson's Disease (PD) is the second most common neurodegenerative disorder in the Western World. Although the majority of cases occur sporadically, several genes have been identified, that, when mutated, lead to familial PD. Of these genetic loci, the Park8 gene encoding a complex, multi-domain protein known as the Leucine-Rich Repeat Kinase 2 (LRRK2), has raised particular interest because of its Roc (Rab) domain. Rab proteins are small GTPases that act as molecular switches in the cell through the cycling of GTP (active) and GDP (inactive). The Rab domain of LRRK2 previously was shown to bind GTP, and so the effects of mutations in this domain were studied in the cell model. It was found that mutations in the Rab domain had a slower rate of GTP hydrolysis when compared to the wild-type, and that an overexpression of these mutations led to neuronal cell death. One mutation in particular had an unusual phenotypic expression in the cell model as well. LRRK2 was previously shown to have kinase activity. Therefore, if the Rab domain within LRRK2 regulates the kinase domain of the protein through GTP hydrolysis, mutations within the Rab domain could make it constitutively active, thereby increasing LRRK2's kinase activity resulting in an unusual cell phenotype that could eventually result in neuronal cell death.

TABLE OF CONTENTS

LIST OF TABLES

LIST OF FIGURES

LIST OF ABBREVIATIONS

ALS	Amyotrophic lateral sclerosis
ATP	adenosine triphosphate
BSA	bovine serum albumin
CHAPS	3[(3-Cholamidopropyl)dimethylammonio]-propanesulfonic acid
CO_2	carbon dioxide
COR	C terminal of Roc
DA	dopamine
DAPK1	death-associated protein kinase 1
ddH_2O	milliQ water, deionized and distilled
DFG motif	Aspartic Acid - Phenylalanine- Glycine motif
DMEM	Dulbecco's Modified Eagle's Medium
DNA	deoxyribonucleic acid
DTT	dithiothreitol
DYG	Aspartic Acid - Tyrosine - Glycine motif
E16.5	Embryonic day 16.5
EDTA	ethylenediaminetetraacetic acid
ER	endoplasmic reticulum
FBS	Fetal bovine serum
G2019S	Glycine substituted by a Serine residue at position 2019 of LRRK2
GABA	gamma-aminobutyric acid

GAP	GTPase activating protein
GDI	guanine nucleotide dissociation inhibitors
GDP	Guanosine diphosphate
GEF	guanine nucleotide exchange factors
GFP	green fluorescent protein
GST	glutathione S-transferase
GTP	Guanosine triphosphate
HCl	hydrochloride
I1371	Isoleucine at position 1371
I2020T	Isoleucine substituted by threonine residue at position 2020 of LRRK2
IPTG	isopropyl β-D-1-thiogalactopyranoside
KCl	Potassium chloride
KOH	Potassium hydroxide
KH_2PO_4	monopotassium phosphate
LRR	Leucine-rich repeat
LRRK1	Leucine-rich repeat kinase 1
LRRK2	Leucine-rich repeat kinase 2
MAPK	mitogen activated protein kinase
MAPKK	mitogen activated protein kinase kinase
MAPKKK	mitogen activated protein kinase kinase kinase
MASL1	Malignant fibrous histiocytomas-amplified sequences with leucine-rich repeats 1

MBP	myelin basic protein
MEM	minimum essential medium
Mg^{+2}	magnesium
$MgCl_2$	magnesium chloride
mRNA	Messenger RNA
NaCl	sodium chloride
NGS	normal goat serum
PAGE	polyacrylamide gel electrophoresis
PBS	Phosphate buffered saline
PCR	polymerase chain reaction
PD	Parkinson's Disease
Pi	inorganic phosphate
PMSF	Phenylmethanesulphonylfluoride
R1398L	Arginine substituted by a Leucine residue at position 1398 of LRRK2
R1441C	Arginine substituted by a Cysteine residue at position 1441 of LRRK2
Rab	Ras protein in brain
REP	Rab escort protein
Roc	Ras of complex proteins
ROCO	Family of proteins containing Roc and COR domains
SDS	sodium dodecyl sulfate
SNpc	Substantia nigra pars compacta

UPS	ubiquitin-proteosome system
WT	wild type
Y1699R	Tyrosine substituted by Arginine residue at position 1699 of LRRK2

ACKNOWLEDGEMENTS

I would like to especially thank Dr Johnny Ngsee for giving me the opportunity to work on this project, and for his encouragement, patience, and advice throughout my Master's experience. I would also like to thank former and present lab members; Dr. Pierre-Yves Gougeon, Derek Prosser, Julie Savaria, Duvinh Tran, and Carine Verly, for their technical and intellectual help, and moral support. Thank you to Rudolfo Zunini and the lab of Dr. Heidi McBride who assisted me with protein purification.

INTRODUCTION

Approximately 100,000 Canadians (roughly 1-2% of the population over age 65) suffer from Parkinson's Disease (PD), the second most prevalent neurodegenerative disorder in the world today [4]. This debilitating disease presents clinical manifestations only after the pathology has reached an advanced stage. At the point of clinical expression, approximately 50% of the dopaminergic cells of the substantia nigra pars compacta (SNpc) and the locus coeruleus of the midbrain are lost resulting in a depletion of striatal dopamine by about 80% [5].

Dopaminergic neurons are found throughout the brain, mostly collected in the midbrain [6]. The role of mesencephalic dopaminergic neurons includes the regulation of voluntary movement as well as influencing reward behaviour. Therefore, a substantial loss of these neurons in the SNpc of the brain leads to PD symptoms which include muscular rigidity, resting tremor, dystonia, dyskinesia, and cognitive disorders [7]. Dopaminergic cell loss leads peripherally to a decrease in tyrosine hydroxylase activity and decreased dopamine in the adrenal medulla, while centrally changes have been observed in both the glutamergic and GABAergic pathways [6]. The main pathological hallmark of PD is severe loss of these neurons in the SNpc and the presence of proteinaceous intracytoplasmic inclusion bodies known as Lewy bodies in surviving cells [8].

PD is a disease of unknown etiology, occurring sporadically almost 95% of the time. The molecular mechanisms underlying the susceptibility of dopaminergic neurons and the regional propensity for cell death are not fully understood, as a variety of mechanisms have been proposed. These include deficits in mitochondrial function and

oxidative stress [9], accumulation of misfolded proteins [10], and the ubiquitin-proteosome system (UPS) dysfunction [11].

A rare 5% - 10% of PD cases have genetic mutations which predispose them to acquiring PD [12]. Some genes have reduced penetrance and are variable at the age of onset, which suggest that although genes may have an impact on PD acquisition, environmental factors must also have a significant influence on the expression of PD. Genetic cases are only a small proportion of total PD cases, but identification of these genes has had a major impact on the understanding of the molecular mechanisms which lead to dopaminergic neurodegeneration [3]. Discovery of these genes for instance, has allowed the construction of animal models with PD to help identify possible targets for therapeutic intervention.

Currently, there are several genetic loci linked with familial PD, some of which are described in Table 1. The detailed phenotypes of these genes vary, but in general, the dominantly inherited genes cause the Lewy body formation disease spectrum, while the autosomal recessive forms cause a milder form of PD with variable inclusion body pathology [13]. This thesis focuses on the Park8 gene, which encodes a protein known as Leucine-Rich Repeat Kinase 2 (LRRK2) expressed in most regions of the brain.

Leucine-Rich Repeat Kinase 2 (LRRK2)

LRRK2 was initially linked to late-onset autosomal dominant PD in the Samighara kindred of Japan in 2002 by Funayama and his colleagues [1]. They identified the gene on the q arm of chromosome 12 (Figure 1A), whereby the primary defect was on the centromeric region of the chromosome, shared by affected and some unaffected individuals suggesting incomplete penetrance [1]. To date, there are over a

Table 1: A list of certain studied genes causing PD.

PARK loci	Gene	Form of Inheritance	Mutation Type	Protein Function	Clinical PD Features
PARK1, 4 (Chromosome: 4q21)	Alpha synuclein, SNCA	Autosomal Dominant	Duplications, triplications, missense: A53T, A30P, G46L	Unknown synaptic function	Usually typical parkinsonism, rapid progression; some mutations have shown cognitive decline, hallucinations, dementia
PARK2 (Chromosome: 6q25.2–q27)	Parkin	Autosomal Recessive, Juvenile	Various mutations, exonic deletions, duplications and triplications	E3 ubiquitin ligase	Early onset resembling idiopathic phenotype, slow progression, levodopa responsive
PARK5 (Chromosome: 4p14)	UCHL1	Autosomal Dominant, idiopathic	Missense: I93M and S18Y	Ubiquitin hydrolase and ligase	Typical parkinsonism
PARK6 (Chromosome: 1p35–p36)	PINK1	Autosomal Recessive	Missense: G309D and exonic deletions	Mitochondrial Serine-Threonine kinase	Early onset, slow progression, levodopa responsive; dystonias and psychiatric features reported
PARK7 (Chromosome: 1p36)	DJ-1	Autosomal Recessive	Homozygous exon, deletion, missense: L166P	Unknown, possible oxidative stress response	Early onset, Levodopa responsive
PARK8 (Chromosome: 12q12)	LRRK2	Autosomal Dominant, idiopathic	Missense including: R1441C/G/H, Y1699C, G2019S I2020T, G2385R	Unknown protein kinase	Usually levodopa responsive typical parkinsonism; certain patients had dystonia, dementia, motor neuron disease

dozen different mutations within the LRRK2 gene which have been identified in unrelated families from various ethnic backgrounds, most of which seem to segregate with PD.

Most LRRK2 families have a clinical phenotype indistinguishable from sporadic PD, yet in patients having the same mutation, different outcomes can arise. For instance, the most common LRRK2 mutation associated with PD is G2019S, as it accounts for 0.7%-1.6% of sporadic cases and 2.8%-6.6% of all familial cases of PD [14]. This mutation has a high frequency in North African Arabs and Ashkenazi Jews [14] but has not been frequently reported in large-scale studies of Chinese PD patients [15] reflecting a possible ethnic influence on acquiring LRRK2 associated PD. Pathological findings in LRRK2 associated PD cases range from pure nigral degeneration without Lewy body formation to typical Lewy body PD [1], which is more common. Therefore, the hypothesis remains that LRRK2 acts as a 'master regulator,' an upstream central integrator of multiple signaling pathways needed for proper neuron function [16].

Although there are these differences, most patients are usually levodopa-responsive [17] to the same extent as sporadic cases. Mutations from LRRK2 associated PD have to date, not been linked with other primary neurodegenerative diseases such as Alzheimer's Disease [18] or Amyotrophic Lateral Sclerosis (ALS) [19].

Specific LRRK2 mutations have been associated with PD, yet other modifier genes, environmental factors, or both, must have an influence on the neurodegenerative process and the varying pathology, since all mutations carriers do not necessarily acquire the disease [15]. Previous studies have shown that G2019S mutation carriers have a higher risk of attaining PD as age progresses, yet some carriers never display a PD

phenotype [19] which may result due to reduced penetrance. Studying the structure of this large multi-domain protein may help understand its function leading to answers to why variable pathology exists with LRRK2 mutant associated PD.

Structure of LRRK2

The LRRK2 gene encodes a 2,527-amino acid protein translated from an approximately 9-kb transcript expressed in most brain regions [3]. It is comprised of 51 exons and has a predicted molecular weight of approximately 286 kDa. This complex protein has multiple conserved functional domains: several leucine-rich ribonuclease inhibitor-like repeats, Roc (Ras of complex proteins) and COR (C terminal of Roc) domains, a catalytic domain of tyrosine kinases, and a WD40 domain [4]. Mutations in the LRRK2 gene have been identified in all domains which segregate with familial, autosomal dominant, late-onset (around 50 years of age) PD (Figure 1B).

LRRK2 has the leucine rich repeat (LRR) domain at the N-terminus end, while the WD40 domain is at the C-terminus of the protein. LRR domains are usually involved in protein-protein interactions including hormone interactions and enzyme inhibition. WD40 domains also are involved in protein-protein interaction, and can be involved in various functions including signal transduction, pre-mRNA processing, and cytoskeleton assembly. These protein interaction domains have led to the assumption that LRRK2 may act as a scaffolding protein.

Next to the LRR domain is the Roc followed by a novel COR domain. These two domains have classified LRRK2 as belonging to the ROCO family [20]. Ras proteins usually act as molecular switches that use GTPase activity to cycle GDP (inactive) for

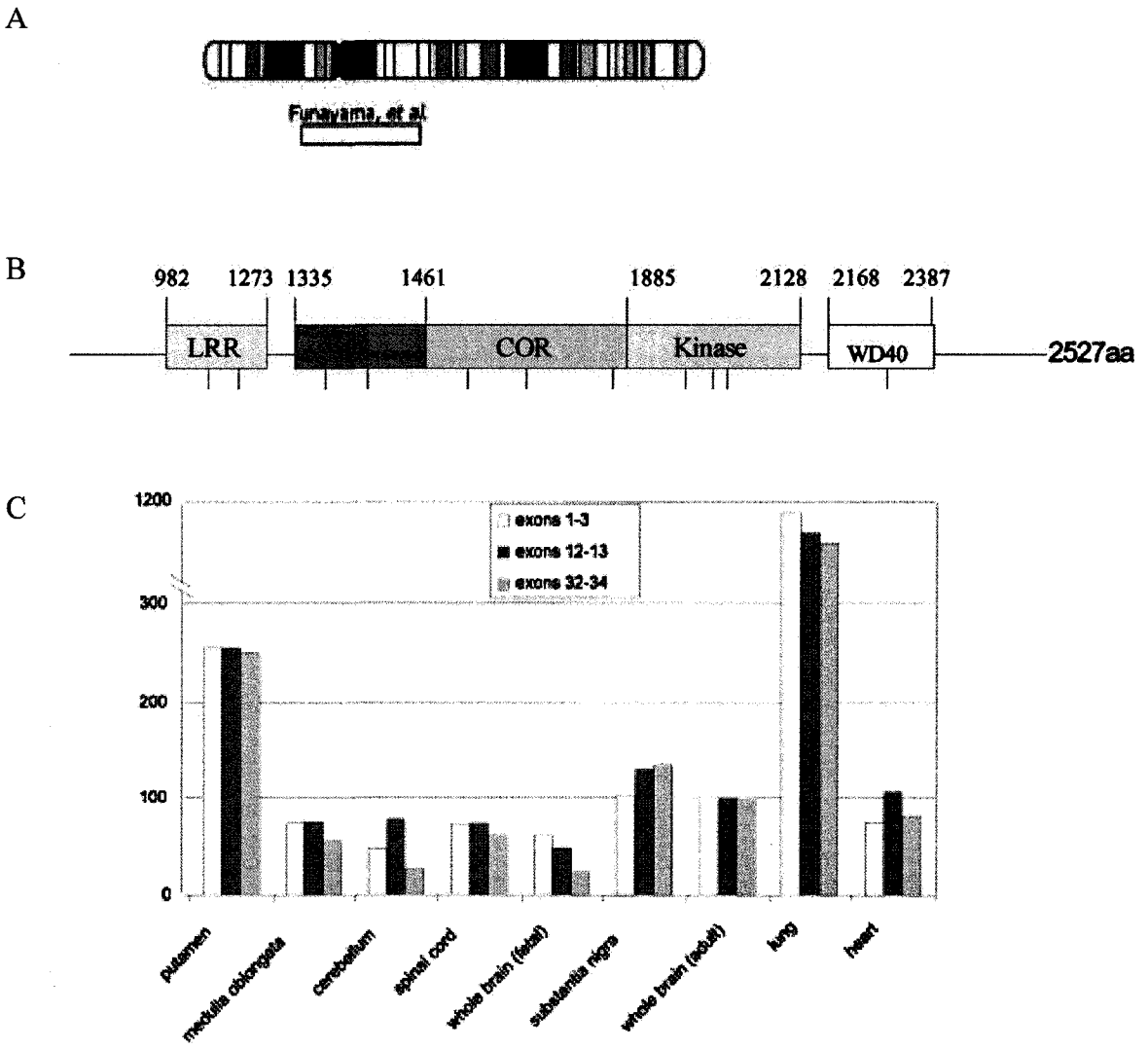

Figure 1: LRRK2 is a complex protein with different domains, expressed in most brain regions.

A. *Ideogram of chromosome 12 (modified from [1]).* Linked areas are shown which were initially defined by Funayama et al. LRRK2 is located on the q arm of this chromosome.

B. *Structure of LRRK2 (modified from [2]).* The gene is 2527 amino acids long containing 5 conserved domains. On the N-terminal is the Leucine-Rich Repeat (LRR) which can be involved in various protein interactions. Next to this domain is the Roc (Ras of Complex proteins) resembling small Ras GTPases, followed by the COR domain which has classified LRRK2 as a ROCO protein. Following the COR is the kinase domain which can activate various phosphorylation events leading to downstream effects in the cell. Finally there is the WD40 domain at the C-terminal end, which like the LRR domain is usually involved in protein interactions.

C. *LRRK2 Expression.* LRRK2 mRNA and protein are detected in most regions of the brain as well as in other areas such as the lungs and heart [3].

GTP (active) to regulate different functions in the cell including kinase activity which can lead to actin cytoskeleton reorganization [21].

In addition to these two domains that give the name "ROCO" to this protein, a third kinase domain is always present in this family suggesting that the three domains are somehow functionally dependent on each other. The kinase domain of LRRK2 belongs to the mitogen activated protein kinase kinase kinase (MAPKKK) subfamily which has catalytic activity on serine/threonine residues and/or tyrosine residues [22]. Kinases are usually involved in phosphorylation as they catalyse the transfer of gamma-phosphate of ATP to residues on protein substrates. To begin to understand the physiological role of this large complex protein and its involvement in PD, it is of great importance to determine when and where the LRRK2 gene is normally active.

LRRK2 Expression

Given the plethora of symptoms and pathologies linking LRRK2 mutations to PD, screening of where the protein is expressed should include not only the brain, but also other parts of the body since autonomic dysfunction is not uncommon in PD. Northern blot analysis revealed that LRRK2 mRNA was expressed in all human tissues, but was most highly expressed in the brain [23]. It was expressed at lower but significant levels in the central nervous system as well as other areas of the body such as the heart, liver, lungs, and kidneys [23] (Figure 1C).

Anatomical mapping studies within the brain (rodent and human) display LRRK2 mRNA as being highly expressed in neuronal cells of dopamine innervated areas including the striatum and caudate putamen [24]. There has been debate however as to whether the LRRK2 gene is expressed in the substantia nigra and within dopamine

neurons, the major cells affected during PD [25, 26], albeit more evidence suggests that there is expression in the substantia nigra. These discrepancies could be due to differences in the sensitivity of techniques used for this analysis.

The LRRK2 protein has been shown in the cortex, striatum, olfactory tubercle, and substantia nigra with similar findings across species of rat, mouse and human [27]. Expression has also been noted in the hippocampus and thalamus, regions not directly associated with typical PD damage, but suggesting a possible involvement of LRRK2 in cognitive and motor aspects of the disease. Within these areas, there is predominant expression in axons, dendrites, and perikarya. Expression levels vary in different regions of the brain, with the higher levels being in the striatum and cortex and lower levels in the substantia nigra and thalamus. When referring to specific neuronal populations that are associated with PD, studies have shown that LRRK2 is highly expressed in dopaminoreceptive areas of the brain such as the medium spiny neurons and interneurons of the striatum. Within these cells, LRRK2 has an intracytoplasmic punctate staining.

In one study, mouse embryonic development was followed with respect to the development of LRRK2. During embryonic development, LRRK2 was detected at E16.5 in the jaw, but not in the brain [28]. LRRK2 was eventually detected in the brain one week after birth at low levels, which increased for the following month until which it reached mature levels of activity [28]. This time course of development parallels the postnatal development of the dopamine innervation of the striatum, which provides further evidence that LRRK2 is involved in this system. Another group found that LRRK2 expression was not typical of a gene important during early development, as they detected the protein later on in pre-natal development and through post-natal

development [29]. Researchers who were able to make a *Drosophila* model of LRRK2 noted that kinase activity was not necessary for the development of dopaminergic neurons [30]. These studies suggest that LRRK2 has an important role in the dopaminergic system, but that its function is not necessarily involved in the development and maturation of developing neurons.

When analyzing the brains of PD patients, it was found that there is a great decrease of dopaminergic cells in the SNpc, which is expected, as this is one of the main pathological hallmarks of PD. However, LRRK2 expression levels were not affected or changes in PD brains detected when compared with normal control samples, or as age progressed either [24]. It should be noted that in this work, the group did not detect LRRK2 in the SNpc but only in dopamine receptive areas of the brain therefore, cell loss in the SNpc did not affect the expression of LRRK2. As to whether or not LRRK2 localizes with Lewy Bodies, another hallmark of disease, there have been contradicting results from different groups [31, 32].

Thus, research to date has shown that LRRK2 resides in areas where dopamine is targeted, within PD associated structures of the brain as well as structures not necessarily associated with PD pathogenesis. Evidence also displays that the protein develops activity in parallel with the innervation of the dopamine system. Determining where it resides in these cells would be of importance in discovering the function of LRRK2.

LRRK2 Localization

The challenge for functional analysis of LRRK2 is its large size and complex domain structure. Groups who have completed *in silico* analysis could not reveal any targeting signal for LRRK2 to specific subcellular compartments, thereby implying a

cytosolic localization [33], which has been confirmed by different researchers through immunocytochemistry [34].

Some collaborations, through subcellular fractionation have found LRRK2 associated with membranes and vesicular structures [33]. The structures that have been connected with LRRK2 are diverse. West and colleagues [36] found that LRRK2 was cytoplasmic most of the time, but about 10% of the protein was found associated with the outer mitochondrial membrane. This could be significant as defects in the mitochondrial pathway (oxidative stress) are one of the leading areas of study thought to lead to PD. Further analysis by Hatano found LRRK2 associated with lipid rafts [35], structures that have important roles in cellular functions such as membrane trafficking, signal transduction, and cytoskeletal organization [35]. Other membranous structures that have been associated with LRRK2 to date include the Endoplasmic Reticulum (ER), the Golgi apparatus, vesicular membranes (synaptic vesicles, lysosomes, endosomes) [38] and the microtubule network. LRRK2 has furthermore been proposed to be within the cytosol of vesicles [36], and to attach to membranes using chaperones [33].

The areas where LRRK2 has been associated could be due to nonspecific antibody labeling of the protein. However, LRRK2 is a multidomain protein and therefore could have different functions within cells. Being associated with different structures is fair to determine where LRRK2 resides. This will help discover its functional activity and its impact on the cell that leads to the pathogenesis of PD.

The Roc domain of LRRK2 resembles Rab proteins which are usually involved in vesicular transport and cytoskeleton assembly or reorganization [20]. Therefore, association with structures such as the ER, Golgi apparatus, and microtubules suggest a

potential importance of the Rab domain within LRRK2 as a regulator of its physiological function. Recently, it was shown that the Roc domain alone can interact with the microtubules [37]. Although PD associated mutations did not necessarily have an effect on the interaction of the Roc domain alone with the microtubules, this interaction could pose a different effect on the entire protein with respect to its kinase activity.

Kinase Activity

The eukaryotic cell is compartmentalized allowing different cellular events to occur simultaneously in specific organelles. Within cells, kinases act as initiator proteins of major signaling cascades such as cell growth, transformation, or apoptosis [38]. These are diverse affects on a cell and therefore, their activity is highly regulated. Usually kinases are compartmentalized in cell regions where they control effector molecules through phosphorylation. They can be controlled through autophosphorylation, by binding activator or inhibitor proteins or small molecules, or by controlling their location in the cell relative to their substrates.

The kinase domain of LRRK2: structural and functional properties

LRRK2 has a kinase domain that, based on phylogenetic analysis resembles the mitogen activated kinase kinase kinase (MAPKKK), a mixed lineage kinase which is catalytic for both serine/threonine and tyrosine [1]. Once activated by extracellular stimuli, cytosolic mitogen activated protein kinases (MAPKs) result in a signaling cascade composed of several phosphorylation events. The MAPKKK phosphorylates mitogen activated protein kinase kinase (MAPKK) which in turn phosphorylates MAPK to result in the cellular outcome. The active site of the kinase domain activation motif is usually flanked by two tripeptide motifs, DFG (DYG in LRRK2) and APE respectively.

In the DFG motif, the D residue is needed to bind Mg^{+2} for ATP transfer while the other residues are required for hydrophobic interactions to allow kinase activity. This site remains inactive until a change in conformation to the activation segment occurs by either phosphorylation or by binding separate regulatory domains. Two mutations within the kinase domain, G2019S and I2020T, are thought to be within the specific activation segment (Mg^{+2} binding site and N-terminal end of the activation loop, respectively [39]) of the kinase domain, both lying in the peptide 'hinge' of a loop that usually covers the catalytic site to prevent substrate access.

LRRK2 was reported to have functional kinase activity by multiple groups [36, 41], as it was shown to autophosphorylate and phosphorylate myelin basic protein (MBP), a generic protein used in phosphorylation assays. Autophosphorylation may be necessary for LRRK2 to regulate itself. These *in vitro* kinase assays have also shown that within the brain, kinase activity is higher when compared to other areas of LRRK2 expression, such as the lungs [40], implying the importance of cell context.

LRRK2 associated PD mutations, G2019S and I2020T, located within the kinase domain, have shown increased kinase activity with respect to the wild type construct [41], by enhancing substrate access to the active site of this domain. Although these reports give an idea of how the kinase domain functions within LRRK2, researchers must be aware that only once the actual substrate being phosphorylated is identified can quantitative conclusions be made about the kinase activity of this protein, and its physiological significance.

The R1441C mutant within the Roc domain of LRRK2 has also shown increased kinase activity using generic substrates for phosphorylation [42]. This finding raises the

question of whether or not the kinase domain is regulated by this Ras-related GTPase domain in LRRK2, which belongs to the family of ROCO proteins.

ROCO Proteins

The ROCO protein super family includes a set of proteins that can either directly or indirectly control kinases. The name "ROCO" comes from the combined term of Roc and COR, which identifies the main domains in these proteins, a Roc domain (Ras of complex proteins), and a COR domain (C-terminal of Roc) [43]. Ras proteins are small GTPases which act as binary molecular switches to regulate diverse cellular processes as they cycle between an active GTP bound state and inactive GDP bound state [44]. The Roc domain is usually preceded by leucine-rich repeats and/or ankyrin repeats both which could be involved in protein-protein interactions [45]. The 300-400 amino acids that constitute the COR domain, whose function is unknown, are usually followed by a kinase domain and WD40 domain [45].

When compared to the Ras superfamily, Roc domains have all the conserved motifs necessary for GTPase activity. Four out of the five loops are conserved with Ras proteins, the only difference in the G4 loop being a histidine in Roc domains that is usually replaced by a lysine group in Ras GTPases [46]. In Ras GTPases, this lysine has a methylene group that provides a hydrophobic surface lying over the purine ring. As a result the histidine group in Roc domains suggests an altered interaction with GTP.

ROCO proteins have been identified in prokaryotes, plants, metazoa, *Dictyostelium*, and recently in humans [46]. Thus far, four ROCO proteins have been identified in humans including LRRK2, leucine-rich repeat kinase 1 (LRRK1) – whose physiological functions are not fully understood --, malignant fibrous histiocytomas-

amplified sequences with leucine-rich repeats 1 (MASL1) – a candidate oncogene --, and death-associated protein kinase 1 (DAPK1) -- a Ca^{+2}/calmodulin regulated serine/threonine kinase that positively influences apoptosis [43]. Apart from the conserved Ras-related GTPase domain, they differ from each other by the presence or absence of different protein-protein interaction modules and a protein kinase domain.

The conserved domain structure and sequence identity of ROCO proteins especially within the Roc, COR, and kinase domains, suggests a common mechanism underlying the function of this family of proteins. LRRK1, although shorter than LRRK2, is its closest paralogue with an identical domain structure based on sequence homology [47]. Naturally occurring mutations within LRRK1 that have been studied thus far, do not lead to PD pathogenesis or other disease phenotypes [47]. It was discovered that this protein had kinase activity which was stimulated upon binding of GTP to its Roc domain [45]. Therefore, LRRK1 was used to study the effects of LRRK2 pathogenic mutants on kinase activity and GTP binding. Results from this study showed that when LRRK2 pathogenic mutations (R1441C and R1441G in the Roc domain, Y1699R in the COR domains, and I2020T in the kinase domain) were constructed in LRRK1, they all bound GTP to the same extent as the wild type but kinase activity was abolished or lowered [45]. These results paved the way to study LRRK2 and understand its molecular function to lead to a better understanding of PD pathogenesis, especially in regards to the Roc domain as an active Ras GTPase.

Ras-related GTPase subfamily: Rab proteins

Ras proteins are small GTPases which act as binary molecular switches to regulate diverse cellular processes such as vesicular transport, cytoskeletal

reorganization, and nucleoplasmic transport. The activation of Ras-related GTPases requires a conversion of the inactive GDP bound state to the GTP bound active conformation (Figure 2A). The binding and hydrolysis of GTP drives a transition among three conformational states: GDP-bound, empty (transitional intermediate), and GTP bound.

Although Ras possesses an intrinsic GTPase activity to catalyze the hydrolysis of the bound GTP to GDP and an intrinsic GDP/GTP exchange activity to cycle back to the active state, these activities are too low to allow rapid GDP/GTP cycling. Thus GDP/GTP cycling is catalyzed by guanine nucleotide exchange factors (GEFs) that act as positive regulators to promote formation of Ras-GTP and GTPase activating proteins (GAPs) that act as negative regulators to cycle Ras back to its inactivate GDP-bound state [48] (Figure 2A).

The LRRK2 Roc domain shares homology with all four groups of the Ras/GTPase superfamily but is most similar to Rab (Ras in brain) proteins which are usually involved in vesicular transport [20]. They are believed to determine the specificity of docking and fusion on intracellular compartments by functioning as signals to assemble machinery controlling those events.

After their synthesis on cytosolic ribosomes, Rab proteins are usually found in their GDP bound, inactive form by the Rab escort protein (REP), with which it forms a complex. This complex is recognized by Rab geranylgeranyl transferase, a prenylation enzyme which transfers geranylgeranyl moieties via thioether linkages to cysteine residues at or near the carboxyl termini [49]. This prenylation step is essential for Rab proteins to tightly associate with the cell membrane [50]. The REP then escorts the

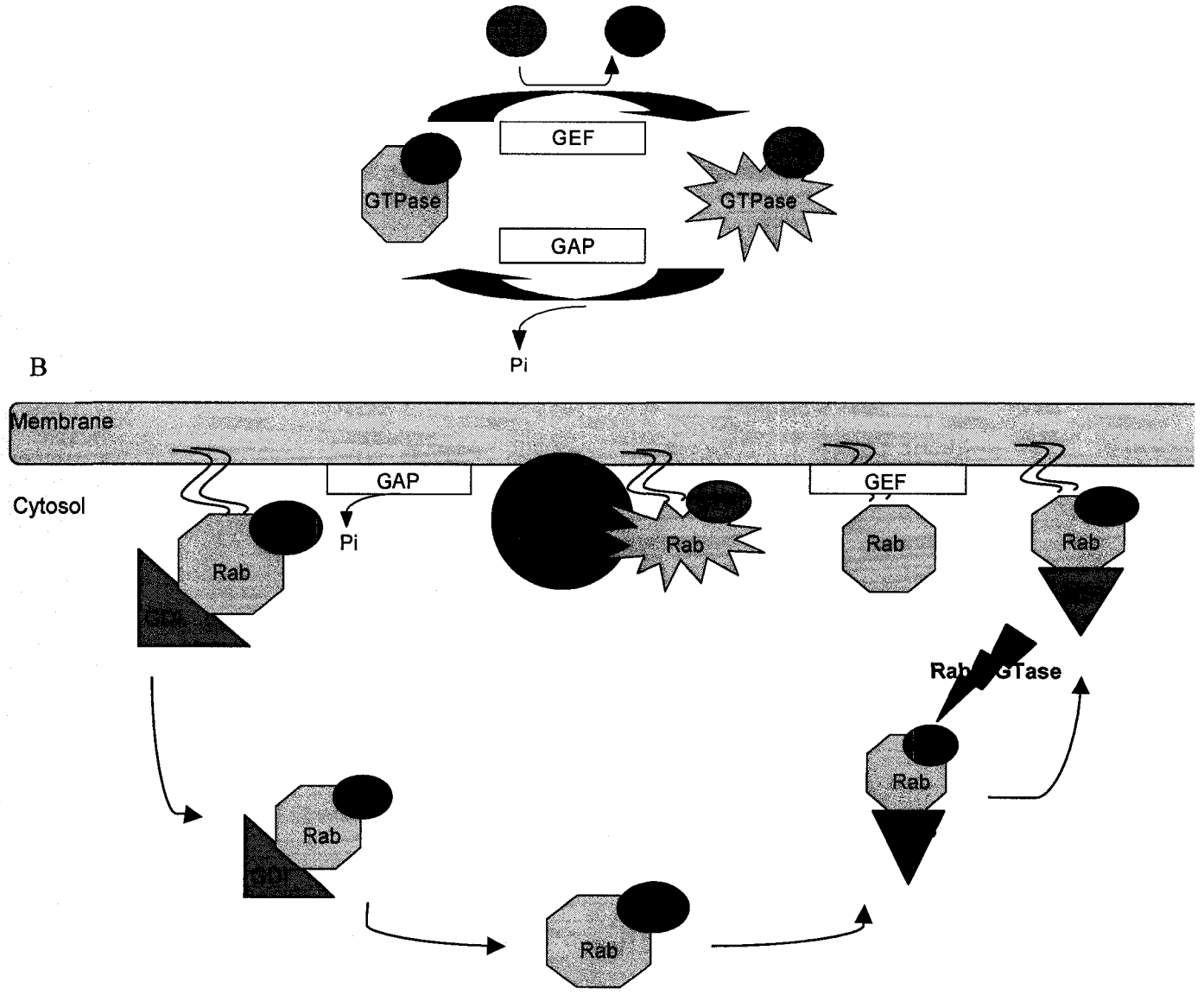

Figure 2: Rab GTPase Hydrolysis Cycle

A. *Small GTPase hydrolysis cycle.* Small GTPases possess very low intrinsic GTPase activity. Therefore GDP/GTP cycling is assisted by guanine nucleotide exchange factors (GEFs) that promote formation of the active form bound to GTP, to cause further downstream cellular events, while GTPase activating proteins (GAPs) catalyse the release of inorganic phosphate (Pi), converting the GTPase back to its inactive state.

B. *Rab GTPase cycle.* In the cytosol, the Rab protein is usually found inactive, bound to GDP by a Rab escort protein (REP), with which it forms a complex, recognized by Rab geranylgeranyl transferase (RabGGTase). RabGGTase prenylates cysteine residues near the carboxyl termini of the Rab, which is escorted by the REP to its target membrane where it binds via the new prenyl groups. Association with a GEF promotes GDP dissociation resulting in a transition into the empty state for a short period whereby GTP binds to the protein as the small GTPase hydrolysis cycle (reviewed in Figure 2A) continues. Activation recruits downstream effectors to the membrane. Once converted to its GDP bound inactive form, the Rab forms a complex with a GDP dissociation inhibitor (GDI) which brings the inactive Rab back to the cytosol until it is later required.

protein to its target membrane where it binds via the new prenyl groups. Association with a GEF promotes GDP dissociation thereby causing a transition into the empty state for a short period whereby GTP binds to the protein resulting in its activation to recruit downstream effectors to the membrane [49]. This interaction regulated by the Rab's intrinsic and catalyzed rates of GTP hydrolysis and nucleotide exchange allows the Rab GTPase to spatially and temporally regulate events such as transport, recycling, endocytosis, and exocytosis [49]. Thereafter the active form is converted through a GAP to its GDP bound inactive form followed by forming a complex with a GDP dissociation inhibitor (GDI) which brings the inactive Rab back to the cytosol until it is later required (Figure 2B).

LRRK2 Roc domain

The crystal structure of the LRRK2 Roc domain was recently discovered to be a unique homodimer [51]. In complex with GDP-Mg^{+2} at 2 Angstrom resolution the Roc domain displays a unique dimeric fold generated by extensive domain swapping that forms a pair of active sites with essential functional groups from both monomers [51]. Two PD associated mutations, R1441 and I1371 are at the interface of the two monomers which must provide specific interactions to stabilize the Roc dimer. Mutations at these sites probably result in the loss of these stabilizing forces thereby indirectly leading to the misregulated GTPase activity when compared with the wild type. A pair of ligand binding sites was identified on the surface of the dimer with well defined grooves for GDP together with a Mg^{+2} metal ion at each site [51]. Dimer interactions are stabilized mainly through hydrogen bonding and hydrophobic interaction outside the nucleotide pocket of the catalytic core.

R1441 mutations are the second most common in LRRK2 associated PD [17]. Through molecular modeling, the R1441 residue of LRRK2 is in a region sharing similarity with the Rab subfamily motif, and through homology suggests that this area may play a possible role in cell localization and protein interactions [20]. The pathogenic R1441 position of LRRK2 is located within the Roc domain on the end of alpha helix 3 which interacts with alpha helix 2 at the dimer interface. The arginine residue is important in stabilizing interactions on the dimer surface as the guanidium group forms hydrogen bonds with backbone residues and helps in the formation of alternating stacks to "produce a hydrophobic 'greasy' zipper across the dimer interface" [51]. Loss of this stabilization due to arginine substitutions for shorter side chains such as cysteine, could result in the displacement of two key residues, R1398 and D1394, needed to interact with the gamma-phosphate of GTP and Mg+2 ion.

The R1398 position in LRRK2 was shown through sequence homology and crystal structures, to be an important residue within the catalytic core of the GTPase domain [20]. A direct comparison of the current Roc structure to Ras bound to a non-hydrolysable GTP analogue, identified R1398 as a key residue that would interact with the gamma phosphate of GTP substrate. Therefore, mutation as R1398L should cause the GTP site to become constitutively active, abolishing its ability to hydrolyze GTP.

As a member of the ROCO family of proteins, LRRK2 has the conserved elements needed for GTP hydrolysis. As a result, several research groups studied the GTP binding and hydrolysis rate of LRRK2. Due to different techniques used, there were contradicting results among the groups. All groups seemed to agree that LRRK2 did bind GTP [52, 53], but while some groups thought LRRK2 had robust GTPase activity [53],

Figure 3: Roc dimer of LRRK2 (NCBI database, **MMDB ID:** 64897)
The Roc domain dimer of LRRK2 shown with the GDP-Mg^{+2} ligands in ball and stick format at binding domain.
In this image, individual monomers are highlighted in pink and blue. The R1398 position lies within the activation segment, therefore mutations possibly interfere with binding of GTP and GDP during hydrolysis. The R1441 position however lies on the surface and therefore mutations in this position that have been associated with PD may indirectly interfere with hydrolysis.

others thought it was very low, or even undetectable [47]. These differences could be due to levels of sensitivity for the different techniques used. The R1441 mutant was found to have a lower hydrolysis rate in comparison to the wild type [53, 54]. It was discovered as well, that the LRRK2 Roc domain was responsible for stimulating kinase activity [53]. This was determined after realizing that the kinase dead mutants had no effect on GTP hydrolysis while mutants in the Roc domain that would abolish GTP hydrolysis rate also led to a non-functional kinase.

This leads to the theory that the LRRK2 Roc is required for the protein to have functional enzyme activity as a kinase. Once GTP is bound to the Roc domain, this activates the kinase domain allowing phosphorylation to lead to downstream effects which can be deactivated once the Roc binds GDP. Mutants in the Roc domain however could cause the kinase domain to misregulate by constitutively activating the Roc domain thereby preventing hydrolysis or could result in an extremely fast turnover rate of GDP for GTP thereby preventing activation of the kinase domain. Thus far however, the first theory seems to coincide with experimental results leading to a hyperactive kinase which could have a downstream effect on its effectors.

LRRK2 overexpression leads to cell death

One downstream effect that seems to result as an overexpression of LRRK2 is neuronal cell degeneration, by means of the active kinase [41]. Through construction of Roc and kinase domain 'dead' mutants, it was shown that the Roc domain is necessary for the kinase domain to remain active while the kinase domain did not require activity for the Roc domain to hydrolyze GTP [53] implying a possible regulatory role, which if altered could cause the effects leading to cell death.

A common feature of neurodegenerative disorders is the loss of neuronal processes early in disease onset. In PD, loss of dopaminergic axons and terminals projecting from the SNpc to the striatum precedes cell death. LRRK2 was shown to regulate neurite process morphology, length and complexity in the mammalian brain [55]. Mutations in LRRK2 leading to PD seem to cause uninhibited kinase activity, a change in neurite length and morphology [55], and eventually cell death [34].

The Roc domain of LRRK2 was found to interact with the microtubules, a cytoskeletal element, which was not altered by PD associated mutations [37]. The internal cytoskeleton of eukaryotic cells is composed of three main types of filaments: microtubules, intermediate filaments, and actin microfilaments, which all help in maintaining cell dynamics and strength. Microtubules play an essential role in the internal cellular organization and localization of the cell organelles including the nucleus and function as a scaffold for internal transport of vesicles and cell organelles. Other PD associated genes (ie. alpha synuclein [56], Parkin [57]) have also been associated with the microtubules, thereby providing further support that they are involved in the PD neurodegenerative process.

Being associated with the microtubules, could imply that there is an impact of LRRK2 with the intermediate filaments as well, since these structures are interconnected. Thus far however, there has not been significant evidence to strengthen this theory. In fact thus far, one study could not confirm a relationship of LRRK2 with the intermediate filaments [33]. This same study however could not detect a relationship with the actin cytoskeleton as well, while another study disagreed, identifying an actin skeletal protein as a possible substrate of LRRK2 [58].

Some ROCO family members have been associated with the cytoskeleton, including DAPk1 which was found to phosphorylate the myosin light chain kinase of the actin cytoskeletal scaffold. Interaction with actin microfilaments is essential for the death promoting activity of this protein [59]. LRRK2 was found to phosphorylate moesin [58], providing further evidence that the protein may be associated the actin cytoskeletal network. Moesin, a member of the ERM proteins (Ezrin/Radaxin/Moesin), helps anchor actin to the plasma membrane and along with radaxin has been shown to have a key role in regulating neurite outgrowth. If determined to be a physiological substrate of LRRK2, this information could suggest that deregulation of moesin phosphorylation by mutant LRRK2 might contribute to the early loss of dopaminergic axon terminals in PD.

LRRK2 Rab Analysis Project Objectives

The data presented suggest that the full length LRRK2 protein is a functional kinase. The Roc domain within this protein regulates the functionality of the kinase, which seems to regulate the morphology of neurite processes. Mutations within the Rab domain therefore that interfere with GTP binding or the structure of the Roc dimer, could lead to a hyperactive kinase domain. This in turn could result in a different phenotype either by decreasing complexity within neurites or by altering cytoskeletal elements within the cell that would eventually lead to cell death associated with PD.

Rab GTPases act as molecular switches cycling between GDP bound (inactive) and GTP bound (active) states. LRRK2 has a Rab domain. LRRK2 was shown to have kinase activity which was regulated by binding of GTP [41] to its Rab domain. Therefore if mutations within the Rab domain cause a change in GTP hydrolysis rate, this could

continually activate the protein's kinase activity and eventually lead to a different cell phenotype resulting in the cell death observed in PD.

Through this study, the effect of Rab mutations (R1441C and R1398L) in LRRK2 was researched. If decreased GTP hydrolysis in the Rab domain leads to enhanced kinase activity, mutations could be the cause of this low GTPase activity. Therefore hydrolysis of GTP by the Rab mutants was compared to the wild type activity. As a result of observing disrupted hydrolysis, these mutations were examined in different cell lines as well to see if they had an effect on cellular expression. Through immunocytochemistry and Western blot analysis, there was no detectable LRRK2 expression in neuronal-like cell lines leading to the hypothesis that these mutants lead to neuronal cell degeneration. This was approached through a cell death assay, confirming this hypothesis, in agreement with the results of Smith and colleagues [34]. This phenotype was examined in the G2019S mutant as well -- which resides in the kinase domain and is the most frequent LRRK2 mutation associated with PD -- leading to the same conclusion. Therefore, the expression of LRRK2 was examined in Chinese Hamster Ovary (CHO) cells, to determine if the Rab mutations along with the G2019S mutation led to differences in cell morphology in comparison to the wild type construct. Immunocytochemistry revealed that the LRRK2 protein could be associated with cytoskeletal elements, and that the R1441C mutant had a unique phenotype in a significant percentage of cells.

MATERIALS AND METHODS

Subcloning and Plasmid Construction

pcDNA3.1(+)myc LRRK2 WT plasmid construction

The LRRK2 WT full length construct was generated by PCR amplification using pCMV6 – XL4/LRRK2 as a template. For mammalian expression, after PCR amplification, the DNA sequence was subcloned into the pcDNA3.1(+) myc vector in several steps.

Nucleotides 1 to 5129 were subcloned as a BamHI/Cla1 fragment into pBluescript II KS (+) after PCR amplification using the following oligonucleotides: 5'-CAC GGA TCC ATG GCT AGT GGC AGC TGT CAG GGG-3' and 5'- TCT CAA GTA ATC GAT TGA TTA ATC TTG ACC-3'. After isolating the BamH1/Cla fragment through *Ultra Clean 15 DNA Purification kit* from MO BIO, it was inserted into the pBluescript vector at the aforementioned cut sites, and the fragment was confirmed in the plasmid by use of the lacZ gene in pBluescript. This gene provides alpha complementation for blue/white color selection of recombinant phagemids. Therefore white colonies were selected and DNA was isolated from these bacterial colonies using the MINI prep kit from Qiagen to confirm that the vector contained the correctly sized insert.

Nucleotides 5130 to 7583 of full length LRRK2 were then amplified as a Cla1/Xho1 fragment using 5'- GGT CAA GAT TAA TCA ATC GAT TAC TTG AGA-3'and 5'- CGA CTC GAG TTA CTC AAC AGA TGT TCG TCT CAT TTT TTC as oligonucleotides from the pCMV6-XL4/ LRRK2 plasmid. This fragment was isolated again through the *Ultra Clean 15 DNA Purification kit* (MO BIO), and inserted into the vector containing the first half of the LRRK2 amino acid sequence, at the Cla1 and Xho1

restriction sites. Confirmation of full length LRRK2 was completed through using the MINI prep kit (Qiagen) to isolate DNA from possible positive clones.

The pBluescript vector now contained the full length LRRK2 sequence. The full length gene was then digested from the BamH1/Xho1 restriction sites, isolated using *Ultra Clean 15 DNA Purification kit* (MO BIO) and cloned into pcDNA3.1(+) myc to be used in mammalian expression, after confirmation that the DNA was in the vector (MINI prep kit, Qiagen).

Site Directed Mutagenesis

Mutations within the Rab domain of LRRK2, particularly, the R1441C mutation has been associated with familial Parkinson's disease. This mutation as well as the R1398L mutation -- which should inactivate GTP hydrolysis -- was generated to see the effect of mutations in the Rab domain of LRRK2 on the cell model.

Mutations for LRRK2 were generated by PCR amplification using pcDNA3.1(+) myc LRRK2 WT as a template. The LRRK2 region between BsrG1 and Pac1 (nucleotides 1710 to 6332) was PCR amplified using 5'- GTA ATT TCT TCT ATT GTA CAT TTT CCT GAT GCA TTA G-3' and 5'- C TTT CAA ACA CTG TTT AAT TAA TTT CTC AAC CAT AGG CC-3' as flanking primers. The R1398L mutation was PCR amplified using the following mutant oligos: 5'-TGG GAT TTT GCA GGT CTT GAG GAA TTC TAT AGT-3' and 5'-ACT ATA GAA TTC CTC ACG ACC TGC AAA ATC CCA-3', while the R1441C mutation was generated with the following mutant oligos: 5'- CAC AGG GGA AGA AGA AGC GCA AGC CTT TAT ATT GAA GAG -3' and 5'- CTC TTC AAT ATA AAG GCT TGC GCT TCT TCT TCC CCT GTG -3'.

The G2019S mutation is the most prevalent mutation associated with Parkinson's disease. This mutation occurs in the kinase domain of LRRK2 and seems to cause a hyperactivity of the kinase domain of LRRK2 [2]. This mutant was also created using the same flanking oligos as when creating the Rab mutations. The oligonucleotide sequences used to create this mutation were as follows: at the 5' end, 5'- GCA AAG ATT GCT GAC TAC AGC ATT GCT CAG TAC TGC TGT -3', and at the 3' end, 5'- ACA GCA GTA CTG AGC AAT GCT GTA GTC AGC AAT CTT TGC -3'. All plasmids were sequenced at the StemCore Sequencing Facility to confirm the expected mutations.

pBUD/eGFP Ce4.1(+) LRRK2 plasmid construction

The pBUD Ce4.1(+) vector contains two promoters; EF-1 alpha and CMV promoters. At the EF-1 alpha promoter, the eGFP sequence had been previously inserted.

LRRK2 WT and mutant constructs were taken from the pcDNA3.1(+) myc vector and inserted into the pBUD/eGFP vector at the Bam HI site following the CMV promoter. The following oligonucleotides were used to PCR amplify the full length LRRK2 insert: 5'-CAC GGA TCC ATG GCT AGT GGC AGC TGT CAG GGG-3' and 5'- CTC TGG ATC CCT CAA CAG ATG TTC GTC TCA -3'. The insert was isolated and purified using the *Ultra Clean 15 DNA Purification* kit from MO BIO and ligated to the vector.

This vector is useful in that following the multiple cloning site, there is a His tag at the C-terminal region of this promoter, therefore allowing it to be bound to Ni-NTA beads.

Construction of GST-LRRK2 Rab constructs

The isolated Rab domain of LRRK2 was constructed by PCR amplification using pcDNA3.1 (+) myc LRRK2 constructs as a template with the following primers: 5'- ATA GAG CTC GGA TCC ATG AAA CTT ATG ATT GTG GGA AAT-3' and 5'- GGC AAG CTT CTC GAG CTA GTC TGG AAT CAG CTG TCC AA-3'. This region corresponds to amino acids 1335–1461 of the LRRK2 Rab domain. The pcDNA3.1(+) myc LRRK2 WT, R1398L, and R1441C constructs were used as templates to generate the corresponding mutations. Each fragment was isolated and inserted into pGEX2T* using the BamHI/Hind III restriction sites in the multiple cloning site of this vector.

Cell Culture

All cells were grown and maintained in 10 cm polystyrene tissue culture dishes (Sarstedt) at 37°C in 5% CO_2, 95% air incubator.

CHO cells

Chinese Hamster Ovary (CHO) cells were grown and maintained in complete alpha MEM (Minimum Essential Medium alpha containing 5% FBS (Fetal Bovine Serum, filter sterilized) and 1% penicillin/streptomycin) (Invitrogen).

HeLa cells

Henrietta Lackman (HeLa) human epithelial cells were grown in complete DMEM (Dulbecco's Modified Eagle's Medium – High glucose (Fisher Scientific) containing 5% filter sterilized FBS and 1% penicillin-streptomycin (Invitrogen)).

B35 Cells

The rat B35 neuronal-like cell line was grown in complete DMEM containing 10% filter sterilized FBS. To seed these cells onto glass coverslips, coverslips were first coated in poly-L-lysine (Roche) because these cells were not as easily able to adhere to glass,

SH-SY5Y cells

The SH-SY5Y cell line is a thrice cloned (SK-N-SH -> SH-SY -> SH-SY5 -> SH-SY5Y) subline of the neuroblastoma cell line SK-N-SH which was established in 1970 from a metastatic bone tumor. These human neuronal-like cells were grown and maintained in a complete 1:1 mixture of DMEM and Ham's F12 media (VWR) containing 10% FBS (filter sterilized) and 1% penicillin-streptomycin (Invitrogen). To seed these cells onto glass coverslips, coverslips were first coated in poly-L-lysine (Roche) because they, like the B35 cell line do not easily adhere to glass.

GTP hydrolysis assay

*Purification of pGEX2T*LRRK2 Rab proteins*

After subcloning the Rab domains of LRRK2 wild type, R1398L, and R1441C mutants into the pGEX2T* vector, the GST-tagged LRRK2 Rab construct proteins were successfully purified from the BL21 codon plus DES (RIL) Escherichia coli strain through binding the GST tag to glutathione sepharose beads (Amersham).

A 1.5% YT + Ampicillin (100 μg/ml) plate was streaked with the bacterial stock containing the pGEX2T*LRRK2 Rab construct of interest, and was incubated overnight at 37°C. The next day, single colonies were selected from the plate and inoculated into 200 ml of sterile 2YT (yeast tryptone) + Ampicillin (100 μg/ml), which were allowed to grow overnight at 37°C in a shaking incubator. The next day, to 900 ml sterile 2YT, ampicillin was added at a final concentration of 100 μg/ml. 100 ml of the overnight culture was added to each flask, and grown at 37°C until the absorbance at 600 nm gave an optical density (OD) reading between 0.6 and 0.8 upon which, cells were induced.

After inducing the bacterial solution using 1 mM isopropyl β-D-thiogalactoside (IPTG) for four hours at 37°C, the bacterial solution was pelleted at 5,000 × g for 10 minutes at 4°C. The cells were then lysed using a French press at approximately 1,500 psi in lysis buffer (25 mM Tris-HCl pH 8.0, 2 mM DTT (dithiothreitol), 2 mM PMSF (phenylmethanesulphonylfluoride)), pelleted at 100,000 × g for 1 hour at 4°C, and the supernatants were bound to equilibrated glutathione beads for 2 hours at 4°C.

The beads were then washed first with a buffer containing 25 mM Tris-HCl pH 8.5, 300 mM NaCl, 0.1% NP-40, and 5 mM beta-mercaptoethanol followed by a wash with 25 mM Tris-HCl pH 8.5, 100 mM NaCl, 0.05% CHAPS, and 5 mM beta-mercaptoethanol. Finally the protein was eluted off the beads using 25 mM Tris-HCl pH 8.5, 100 mM NaCl, 0.05% CHAPS, 25 mM glutathione, 5 mM beta-mercaptoethanol, which was titrated to a pH of 8.5 with 2 M NaOH. For each protein construct, 10 L of bacteria were prepared.

Phosphate Standard

A 0.5 M KH_2PO_4 (VWR) stock solution was made in ddH_20 to generate a standard curve of Pi released: from this 0.5 M stock a 1:100 dilution in ddH_20 was made to yield a 5000 μM Pi stock. A 1:10 dilution of this stock was used to create a working stock of 500 μM Pi stock, from which dilutions were made in GTPase assay buffer (20 mM Hepes-KOH pH 7.5, 150 mM KCl, 2 mM $MgCl_2$, 1 mM DTT) to create the standard solutions.

Basal GTPase Assay (modified from [60])

Each Rab protein was diluted to twice its final concentration (2 μM) in GTPase assay buffer (20 mM Hepes-KOH pH 7.5, 150 mM KCl, 2 mM $MgCl_2$, 1 mM DTT).

GTP (Roche) was also diluted to twice its final concentration (0.5 mM) in GTPase assay buffer.

To initiate the reaction, 200 µl of the GTP stock was added to 0.6 ml eppendorf tubes containing 200 µl of the Rab protein stock, mixed quickly, and transferred to a 37°C water bath. Before transfer however, a 20 µl aliquot was removed as a negative control, and transferred to microtiter wells containing 5 µl of 0.5 M EDTA (ethylenediaminetetraacetic acid) (pH, 8.0) (Sigma). 100 mM EDTA immediately halts the reaction by chelating the Mg^{+2} needed for GTP hydrolysis. This was done in triplicate.

Every 30 minutes, 20 µl aliquots were taken in triplicate and added to the microtiter wells containing 100 mM EDTA for up to 150 minutes. When the time course was completed, 150 µl of a Malachite Green Stock Solution (1 mM Malachite Green, 10 mM ammonium molybdate in 1 M HCl (34 mg Malachite Green Carbinol base (Sigma), was dissolved in 40 mL 1 M HCl. 1 g ammonium molybdate tetrahydrate (Sigma) was dissolved in 14 mL 4 M HCl. The two solutions were mixed and brought to 100 mL with distilled water, which was then filtered though a 0.2 µ Nalgene filter (VWR) and stored at 4°C in the dark.)) was added to each well and the absorbance was read at 650 nm using a microplate reader. A standard curve from 25 µM to 300 µM Pi was generated for each experiment and read in parallel after adding 150 µl Malachite Green Stock Solution to all the wells.

LRRK2 Expression

LRRK2 Expression using Immunocytochemistry

To look for expression of the LRRK2 protein, cells were seeded at a density of $8x10^4$ cells/ml onto sterile 12 mm glass coverslips (Fisher) which were in 24 well dishes (VWR, Nunc). The next day, cells were transfected with 400 ng pcDNA3.1(+) myc LRRK2 DNA per well using Lipofectamine Reagent (Invitrogen) to aid in transfection. For one well, the transfection was completed as follows: 400 ng LRRK2 DNA was diluted in 50 µl Opti-MEM (Gibco), and in a separate 0.6 ml eppendorf tube, 1 µl Lipofectamine Reagent was diluted in another 50 µl Opti-MEM (per well). These solutions were mixed together and kept at room temperature allowing the DNA to bind the lipid complex for 30 to 40 minutes. The cells that were previously seeded, were washed with 0.5 ml PBS and 200 µl Opti-MEM replaced the media. The lipid:DNA solution was then overlayed onto the cells which were incubated at 37°C for 4 hours, after which the transfection was halted by replacing the serum free media with complete MEM.

Approximately 48 hours after transfection, cells were fixed onto the coverslips using 4% paraformaldehyde in PBS (phosphate buffered saline) for 30 to 60 minutes. Cells were then rinsed in 0.1 M glycine in PBS (containing 0.01% sodium azide to prevent bacterial contamination), and blocked in blocking buffer (1% BSA (bovine serum albumin), 2% NGS (normal goat serum), 4% saponin, and 0.01% sodium azide in PBS) for 30 minutes. Buffer was replaced with the mouse anti-myc primary antibody diluted in blocking buffer for 1 hour at room temperature. Cells were again rinsed in 0.1 M glycine in PBS, blocked in blocking buffer for 30 minutes, and secondary antibody,

Alexa 488 goat anti mouse, was added in blocking buffer to the fixed cells. Incubation time was for 1 hour at room temperature in the dark, after which cells were washed with 0.1 M glycine in PBS, neutralized with equilibration buffer (Invitrogen), and mounted onto slides using the Slow Fade Reagent from Invitrogen. This was done in CHO, B35 and SH-SY5Y cell lines.

LRRK2 Expression through harvesting cells and binding to Ni-NTA beads

Being unable to detect expression of the myc LRRK2 signal in neuronal-like cell lines through immunocytochemistry, a different approach was used by taking advantage of the His tag in pBUDCe4.1(+) LRRK2 constructs.

To make sure the experiment was reliable, this approach was first tested in CHO cells, since low expression was seen with immunocytochemistry. Cells were seeded at a density of $1.5x10^6$ cells/ml into 4 separate 10 cm polystyrene dishes (Sarstedt). Each plate of cells was transfected the next day with 5 μg pBUD/eGFP/LRRK2 DNA and 7.5 μl Lipofectamine Reagent in OptiMEM for 4 hours at 37°C, after which the transfection media was replaced with growth media. 4 plates of cells with the empty vector, pBUD/eGFP were managed in parallel as a negative control.

Forty-eight hours after transfection, cells were scored by counting the amount of GFP positive cells in a field of view containing at least one hundred cells to determine the transfection efficiency. Once this was completed, the cells were harvested in PBS at room temperature. Each plate was scraped in 0.5 ml PBS using a rubber policeman and the cells were collected into two 1.6 ml eppendorf tubes (2 ml per DNA construct). Triton X-100 and PMSF were added to each tube at a final concentration of 1% and 2 mM respectively. The tubes were then kept on ice for 20 minutes during which time they

were mixed intermittently. Insoluble material was then spun out at 21,000 x g at 4°C for 10 minutes. The supernatant from each tube was added to 20 µl of equilibrated Ni-NTA beads (Qiagen), which was incubated for 2 hours at 4°C to allow the His-tagged protein to bind to the nickel beads.

Finally, the beads were spun out, pooled into one tube (40 µl beads total), and washed three times with PBS (VWR) containing 0.5% Triton X-100 (The first flow through was kept at -80°C in case the protein did not bind to the beads for any reason)

40 µl sodium dodecyl sulfate (SDS) sample buffer was added to the beads, and the samples were boiled at 100°C for 10 minutes. They were then loaded onto a 6% SDS-PAGE gel and run using the Western apparatus. The gel was transferred for 2 hours onto nitrocellulose paper which was then blocked in 5% blocking buffer (0.15 M NaCl, 0.01 M Tris-HCl, pH 7.5, 5% skim milk) for 30 minutes. The blot was probed with mouse monoclonal anti-myc primary antibody (Stressgen) overnight at 4°C in the dark at a dilution of 1:1000 and washed in Western Wash Buffer (0.15 M NaCl, 0.01 M Tris-HCl, pH 7.5) three times; once for 10 minutes and twice for 5 minutes. The blot was then probed with Alexa 488 goat anti-mouse (Invitrogen) secondary antibody at a 1:2000 dilution for one hour at room temperature in the dark. It was washed again as previously described and developed. This was repeated in the B35 and SH-SY5Y cell lines to see if LRRK2 was expression could be detected in these cell-lines as well.

Trypan Blue Assay

Using immunocytochemistry and Western blot analysis, there was no detectable LRRK2 expression in neuronal-like cell lines. Therefore the Trypan Blue assay was

completed to see if the cells were dying over time which would explain why a LRRK2 signal was not distinguishable.

CHO, B35, and SH-SY5Y cells were seeded into 48 well polystyrene dishes at densities of $3x10^4$ cells/ml, $4x10^4$ cells/ml, and $4x10^4$ cells/ml, respectively. Due to the large size of the HeLa cells, they were seeded into 24 well polystyrene dishes at a density of $2x10^4$ cells/ml.

The next day the cells were transiently co-transfected with 200 ng pcDNA3.1(+)myc LRRK2 constructs and 50 ng pEGFP, using Lipofectamine Reagent (Invitrogen) to aid the DNA in reaching the nucleus. For one sample, DNA was diluted in 25 µl OptiMEM (Gibco) in 0.6 mL eppendorf tubes while 0.5 µl Lipofectamine Reagent was diluted in 25 µl OptiMEM. The solutions were mixed allowing the lipid and DNA to bind at room temperature for 30 to 40 minutes. The cells which were seeded previously were washed with 250 µl PBS (VWR), and 150 µl OptiMEM was added to each well. The cells were overlayed with the transfection mixture, and incubated for 4 hours at 37°C allowing the DNA to enter the cell's nucleus. After 4 hours, the OptiMEM was replaced with the 0.5 ml growth media, and cells were kept at 37°C overnight. A 0.4% Trypan Blue (Sigma) solution was prepared in the appropriate growth media (depending on cell type), and filter sterilized. One day after transfection, 180 µl growth media replaced the existing media of the cells and 20 µl 0.4% Trypan blue was added to each well (1:10 dilution). Cells were observed under fluorescent microscope in search of GFP positive cells, and under white light transmission to identify from the GFP positive cells, those that were Trypan Blue positive. Once the cells were counted, the media was

replaced with the growth serum, incubated overnight, and scored again the following two days.

LRRK2 Co-localization Analysis

After seeing the expression of LRRK2 in the CHO cells, determining whether the protein was associated with a particular subcellular structure through immunocytochemistry became intriguing. Cells were maintained as described in *LRRK2 Expression using Immunocytochemistry*. Staining with the different primary and secondary antibodies was the only difference. The paraformaldehyde-fixed cells were incubated with blocking buffer containing 2 primary antibodies – one to detect the myc signal (LRRK2) and the other to label the subcellular structure of interest. Incubation times were the same, 1 hour at room temperature. Cells were then rinsed as previously completed, in 0.1M glycine in PBS, blocked in blocking buffer for 30 minutes, and buffer diluting 2 secondary antibodies was added to the fixed cells for 1 hour at room temperature in a dark atmosphere. Secondary antibodies can be conjugated to fluorescent agents so that they can be viewed and distinguished through fluorescence microscopy. They recognize immunoglobulins of a particular species which allows detection of the primary antibody. For instance, when trying to determine LRRK2 co-localization with the Golgi apparatus, one primary antibody is required to recognize the myc epitope of LRRK2. The other antibody should detect an antigen in the Golgi apparatus (i.e. Mannosidase II), but would have to be raised in a species different from that of the myc antibody so that the two proteins could eventually be differentiated (i.e. mouse anti myc, rabbit anti Mannosidase II). These two species are detected by two different secondary antibodies (one recognizing rabbit and the other, mouse), which are distinguished

Table 2: List of Antibodies used for Immunocytochemistry to Analyze Cell Structures.

Cell Structure	Antibody	Dilution
Early Endosomes	Rabbit anti- EEA1	1:100
Endoplasmic Reticulum	Rabbit anti-calreticulin	1:200
Golgi Apparatus	Rabbit anti-Mannosidase II	1:200
Mitochondria	Mouse anti-cytochrome c	1:500
Microtubules	Mouse anti alpha tubulin	1:200
	Mouse anti acetylated tubulin	1:200
Intermediate Filaments	Mouse anti vimentin	1:250
LRRK2	Mouse anti-myc	1:1000
	Rabbit anti-myc	1:100

because they are bound to agents which emit light at different wavelengths (usually red (594 nm) or green (488 nm)), which can be detected by fluorescence microscopy

The different subcellular structures that were analyzed with LRRK2 are listed in Table 2, along with their corresponding antibodies and dilutions that allow their detection using confocal microscopy. The myc antibodies used to detect myc LRRK2 are also listed in this table. This process was repeated in the B35 and SH-SY5Y cell lines to look for LRRK2 expression, however no LRRK2 positive cells could be found even if cells were fixed 16, 24, or 36 hours after transfection.

LRRK2 R1441C morphology analysis

In the CHO cell line, the R1441C mutant had an unusual filamentous cage-like morphology in some cells. To determine whether or not this was a striking phenomenon, LRRK2 transfected cells were counted for this mutant as well as the wild type and other mutant constructs. Of the transfected cells, cells that had the filamentous morphology were scored versus those that had the usual punctate phenotype.

Colchicine Treatment

Colchicine Test Assay

In the CHO cell line, there seemed to be slight co-localization of LRRK2 with the microtubules and vimentin (especially of the R1441C mutant with the filamentous morphology). This raised the question that if the microtubules were de-polymerized with colchicine, was there a change in the structure of the intermediate filaments in transfected cells.

This test assay was used to determine an appropriate concentration at which to use colchicine to cause depolymerization of the microtubules. A stock culture of colchicine

(Sigma) was made at 10 mg/ml in PBS, pH 7.4, filter sterilized, and kept at -20°C until required. Three different concentrations -- 1μg/ml, 4μg/ml, and 10μg/ml -- were made in MEMc to use in this test assay (determined based on information from previous research [61-63]) at different time points (2 hours, 4 hours, 8 hours, 24 hours) to determine an adequate concentration to depolymerize the microtubules without causing cell toxicity.

CHO cells were seeded into onto 12 mm glass coverslips (2 mm) at a density of $1x10^5$ cells/ ml. The next day, cells were washed with 0.5 ml PBS and complete MEM with the different colchicine concentrations overlayed the cells at 37°C. After incubating the cells at 37°C for 2 hours, 4 hours, 8 hours, and 24 hours, cells were fixed onto the coverslips. Two wells were used for each condition (colchicine concentration and incubation period); one to label the microtubules to make sure they were depolymerized, and one to label intermediate filaments to see if there was a change in their structure when colchicine was added. As a negative control, complete MEM without colchicine was added to two coverslips to compare the microtubule and intermediate filament structures to cells that were treated with colchicine.

After cells were paraformaldehyde fixed for 1 hour at room temperature at the 2, 4, and 8 hour time points, they were rinsed with PBS, put on blocking buffer at 4°C, and finally kept in primary antibody (mouse anti-alpha tubulin at 1:200 to label the microtubules, or mouse anti-vimentin at 1:250 to label the intermediate filaments) overnight at 4°C. After 24 hours, the final time point for each concentration was fixed and rinsed as the other coverslips, blocked for 30 minutes at room temperature, and put on primary antibody for 1 hour at room temperature. Then all coverslips were rinsed, blocked, and put on secondary antibody (Alexa 488 anti-mouse, 1:500) for 1 hour at

room temperature, and mounted onto slides. Cells were viewed using confocal microscopy to determine an appropriate concentration to use (Figure 15).

Colchicine Treatment

After conducting the colchicine test assay, it was determined that a concentration of 1 μg/ml was sufficient to depolymerize the microtubules after 24 hours, and cause a change in the structure of the intermediate filaments. CHO cells were seeded onto 12 mm glass coverslips at a density of $8x10^4$ cells/ml and were transfected the next day with 400 ng pcDNA3.1(+) myc LRRK2 constructs using Lipofectamine as a transfection reagent (transfection was completed as described in *4.3a LRRK2 expression*). The following day, media was replaced with media containing 1 μg/ml colchicine (final concentration), which was kept on the cells for 24 hours at 37°C. After 24 hours, cells were fixed onto the coverslips using 4% paraformaldehyde in PBS, stained with rabbit anti myc (1:100) and mouse anti-tubulin (1:200) or mouse anti-vimentin (1:250) for 1 hour at room temperature. Coverslips were then rinsed, blocked, and incubated with secondary antibodies (Texas red goat anti- mouse (1:500) and Alexa 488 goat anti rabbit (1:300)) for 1 hour at room temperature. They were finally rinsed, equilibrated, and mounted onto slides using SlowFade Reagent (Invitrogen) to help prevent in degradation of the fluorescent signal from the secondary antibody.

RESULTS

Mutations within the Rab domain of LRRK2 alter intrinsic GTP hydrolysis rate.

The Rab domain within LRRK2 sparked interest as a possible regulator of the protein's kinase activity, as it was previously shown to bind GTP and GDP [41]. Since Rab proteins act as molecular switches to regulate cell processes through the cycling of GDP and GTP, mutations within this domain could alter this regulation process. In LRRK2, mutations within the Rab domain could lead to altered GTP hydrolysis rates, which in turn could affect its kinase activity. The main focus of this work was on mutations within the Rab domain: R1441C -- associated with PD, and R1398L – an artificial construct created based on sequence homology, which manipulates critical residues in Rab that participate in GTP binding and hydrolysis. This construct was generated for comparison, to eventually determine whether the R1441C mutant resulted in decreased GTPase activity.

After subcloning the Rab domains of LRRK2 wild type, R1398L, and R1441C constructs into the pGEX2T* vector, the GST-tagged LRRK2 Rab protein constructs were successfully purified through binding the GST tag to glutathione sepharose beads. The proteins were then used in a colorimetric micromethod GTP assay to determine the amount of inorganic phosphate (Pi) released over time, using the basic dye, Malachite Green, as an enhancer. Sensitive colorimetric assays for inorganic phosphate are based on the formation of a colourless phosphomolybdate complex at low pH. In the presence of an enhancer, like Malachite Green, it is converted to a coloured complex. In acidic solution the complex is a brownish-yellow as it is converted into its respective cation, while it is usually a brilliant green in basic solutions.

This GTP hydrolysis assay is based on the formation of a complex between malachite green molybdate and free orthophosphate that absorbs at 620-650 nm, which can be quantified spectrophotometrically. Upon addition of GTP into a solution containing the Rab protein construct and magnesium ions, GTP hydrolysis was allowed to progress. The reaction was halted using EDTA at several time points, which chelates magnesium blocking further hydrolysis. The assay was completed for each construct at least three times.

Over time, there was a slow rate of Pi released suggesting GTP hydrolysis in the wild type LRRK2 Rab construct, at 0.1695 μM phosphate/min/μM Rab, while there was much slower hydrolysis rates in the R1398L (0.0780 μM phosphate/min/μM Rab), and R1441C (0.0704 μM phosphate/min/μM Rab) mutants (Figure 4). Statistical values obtained through conducting an Analysis of Variance (ANOVA) followed by the Tukey-Kramer post hoc test to check for differences between groups showed that in comparison to the wild type construct, the hydrolysis rates of two mutant constructs were significantly different ($p<0.001$). There was no significant difference in the rates of hydrolysis between the two mutants. The slower hydrolysis rates due to the LRRK2 Rab mutant constructs raised interest in the physiological effects of the full length LRRK2 wild type and mutant constructs in mammalian cell lines.

Overexpression of LRRK2 leads to neuronal cell degeneration

In order to study the physiology of LRRK2 in mammalian cell lines, protein expression was first explored. Other groups had found LRRK2 expressed ubiquitously throughout many organs of the body such as the heart and lungs, but most highly in the

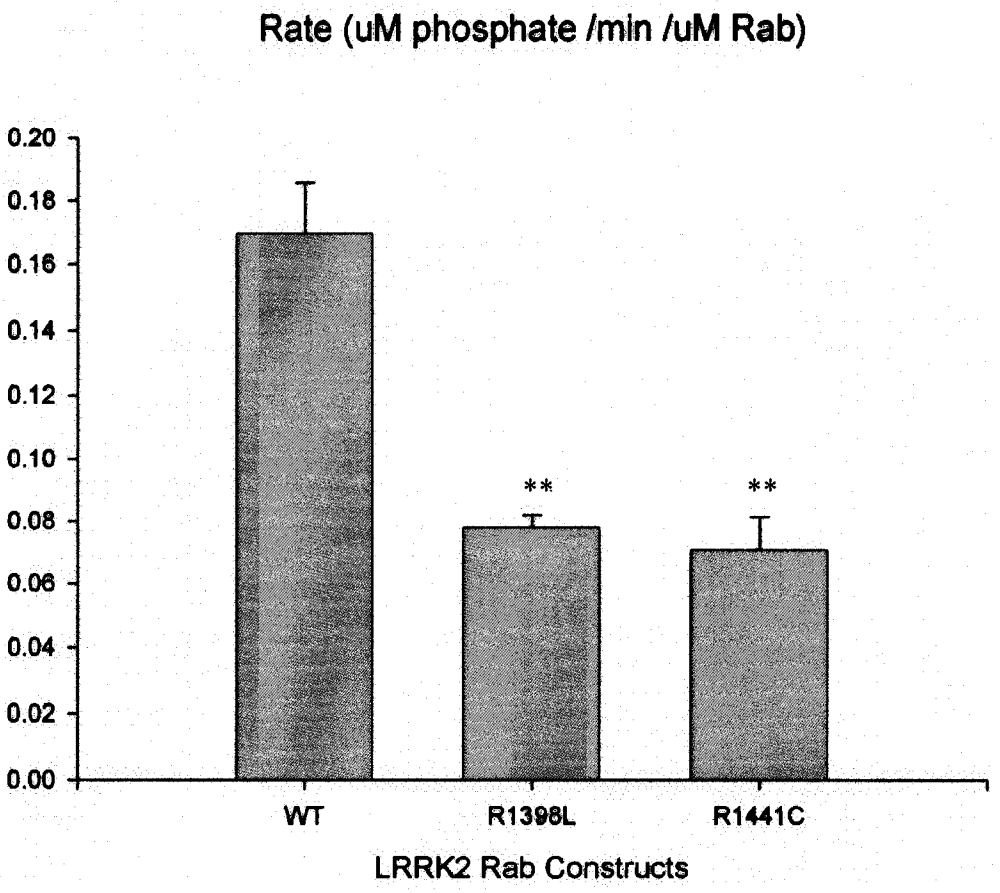

Figure 4: Intrinsic GTP Hydrolysis Rates of LRRK2 Rab wild type (WT) and mutants. pGEX2T*LRRK2 Rab protein constructs (WT, R1398L, R1441C) were purified and used in a colorimetric GTP assay which detects amount of inorganic phosphate released into solution by a change in complex formation. Over time, there was a slow rate of hydrolysis by the wild-type construct and even slower rates by the mutant constructs (** represents $p<0.001$).

brain [5]. In PD, since neuronal cells are most affected, immunocytochemistry was conducted to determine where and how the protein was expressed in mammalian neuronal-like cell lines.

LRRK2 expression is undetectable in neuronal-like cell lines

The full length LRRK2 wild type and mutant cDNA were subcloned into the pcDNA3.1(+) myc mammalian expression vector, transfected into different cell lines, and analyzed through immunocytochemistry. Two neuronal-like cell lines (human SH-SY5Y and rat B35) were transfected but to no avail, as no LRRK2 myc signal was detectable to confirm expression. The low expression levels were indistinguishable from background signal, even if transfected cells were fixed 16, 24, or 36 hours after transfection. A faint signal however was found in the CHO fibroblast-like cell line through immunocytochemistry. As a result, these CHO cells were transfected with the LRRK2 wild type and mutant constructs and analyzed to see if there was co-localization with subcellular structures through further immunocytochemistry and confocal microscopy.

Immunocytochemistry was unsuccessful in showing myc LRRK2 expression in both neuronal cell lines. Therefore, the faint myc LRRK2 expression levels detected in the CHO line through immunocytochemistry were explored by enhancing the myc LRRK2 signal and quickly purifying and concentrating the proteins, to analyze through Western blotting. The LRRK2 full length constructs from pcDNA3.1(+) myc were subcloned into pBUDCe4.1(+)/eGFP which has a 6xHis tag at the C-terminus allowing protein purification through binding Ni-NTA beads. Forty-eight hours after transiently transfecting CHO cells and B35 cells with the pBUD/eGFP/LRRK2 constructs, the

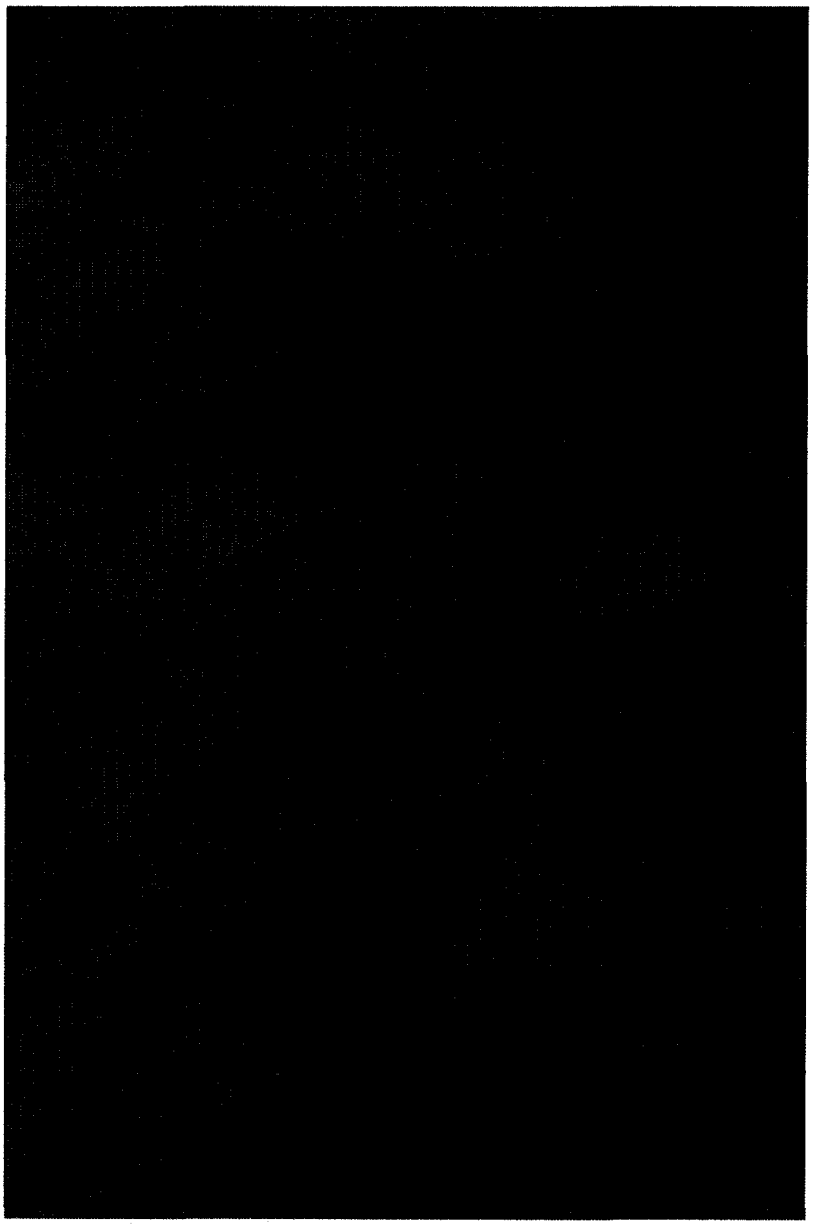

Figure 5: LRRK2 Expression in CHO cells using Western Blot Analysis.
CHO cells were transiently transfected with either pBUD/eGFP vector only (as a negative control) or pBUD/eGFP containing full length LRRK2 constructs (wild type, R1398L, and R1441C). The pBUD vector, containing a His tag, allows transfected cells to bind to Ni-NTA beads after being harvested. Samples were run on a 6% SDS-PAGE gel and probed with mouse anti-myc (1:1000) to detect the band around 286 KDa corresponding to the size of full length LRRK2. This experiment was also done in the B35 cell line but no 286 KDa band was detected.

cells were harvested, bound to Ni-NTA beads using the His tag of the vector, and run on a SDS-PAGE gel. There was a weak band running just above the 250 kDa marker corresponding to the size of LRRK2 (286 kDa) (Figure 5) in the CHO cells but this was not seen in the neuronal-like cell lines.

LRRK2 overexpression leads to neuronal cell degeneration

The low to undetectable expression levels of LRRK2 in neuronal cell lines could be due to many reasons, including cell death. There was previous evidence showing that overexpression of LRRK2 causes neuronal cell degeneration [34]. As a result of these findings, cell survival was studied in different cell lines, through a Trypan Blue assay.

The assay was conducted after co-transfecting cells with pcDNA3.1(+)myc/LRRK2 constructs and pEGFP. Trypan Blue stains dead cells blue, as it penetrates through the pores of the disintegrating plasma membrane of dead cells, which can not be accomplished in live cells due to their intact plasma membrane. In this assay, the LRRK2 transfected cells were identified by GFP fluorescence and cell viability was assessed by Trypan Blue exclusion. The number of dead cells was subtracted from the amount of total GFP positive cells to determine the number of surviving transfected cells. This was repeated for the next two days to determine if cells were surviving or dying after LRRK2 transfection over 3 days. This procedure was completed for each LRRK2 construct at least 3 times in each cell line.

Overexpression of LRRK2 led to a decrease in cell survival over time in the neuronal-like cell lines, SH-SY5Y and B35, but did not have an effect in fibroblast-like cell lines, CHO and HeLa, as these cell lines replicated at a consistent rate over time (Figure 6). All data was standardized to Day 1, to determine if cells were replicating over

time. For statistical comparisons, control, LRRK2 wild type, and LRRK2 mutant data were compared for each day, through an ANOVA followed by the Tukey-Kramer post hoc test. In the epithelial-like cell lines, HeLa and CHO, LRRK2 transfected cells grew at a consistent rate up to day 3 without much difference from the control group (cells co-transfected with the empty pcDNA3.1(+) myc vector and pEGFP) or when compared to each other ($p > 0.05$). When LRRK2 was transfected into the B35 neuronal-like cell line, there was no significant difference in cell survival on Day 2 among control, wild type, and R1398L LRRK2 constructs. However, there was a significant difference ($p < 0.05$) in cell survival in the R1441C mutant when compared to the control. In analysis of Day 3 values, there was no significant difference when comparing the control group to the wild type construct ($p > 0.05$), but there was a striking difference in cell survival when compared to the R1398L constructs ($p < 0.05$), and an extreme difference when compared to the R1441C mutant ($p < 0.001$). When LRRK2 constructs were compared to each other, there were no striking differences between groups ($p > 0.05$).

When analyzing the SH-SY5Y survival rate, on Day 2, the LRRK2 constructs did not have notable differences between groups. When compared to the control there was not much difference from the wild type and R1398L, but as in the B35 cell line, there was a significant difference when compared to the R1441C mutation ($p < 0.05$). On Day 3, there was again no difference among LRRK2 constructs, but when comparing control to the wild type construct, there was a significant difference ($p < 0.05$), not observed in the B35 cell line. When evaluating the differences between the control and Rab mutants (R1398L, R1441C), results were significant ($p < 0.001$).

The results from this assay can lead to the assumption that expression of LRRK2 Rab mutants lead to neuronal cell degeneration. Therefore, the G2019S mutant was also transfected into cells to see if this mutant produced the same phenotype as the Rab mutations. This construct is the most prevalent mutation associated with LRRK2 associated PD [14], found in the kinase domain of the protein. If this mutation was involved in the same pathway as the R1441C mutation which is also associated with PD, it would be expected that this mutant would produce the same outcome as the R1441C mutant.

As with the other LRRK2 constructs, in both epithelial-like cell lines, LRRK2 G2019S transfected cells grew at a consistent rate up to Day 3 without much difference from the control group (empty vector) or from the other LRRK2 constructs ($p > 0.05$). In the B35 neuroblastoma cell line, there was no significant difference when comparing growth on Day 2 between control and the LRRK2 G2019S constructs, but by Day 3, values were strikingly different when comparing control to the G2019S construct ($p < 0.05$). There was no difference however between LRRK2 constructs ($p > 0.05$). When studying the SH-SY5Y survival rate, on Day 2 there were no notable differences between LRRK2 constructs or when the construct was compared to the control. On Day 3, there was again no interesting difference among LRRK2 constructs, but when comparing control to the G2019S mutant construct, there was a significant difference ($p < 0.05$). This response was consistent with the data obtained for the R1398L mutant, but was different from the R1441C mutant which led to a greater degree of cell death in the neuronal cell lines. These findings made determining the expression and localization of LRRK2 even more interesting.

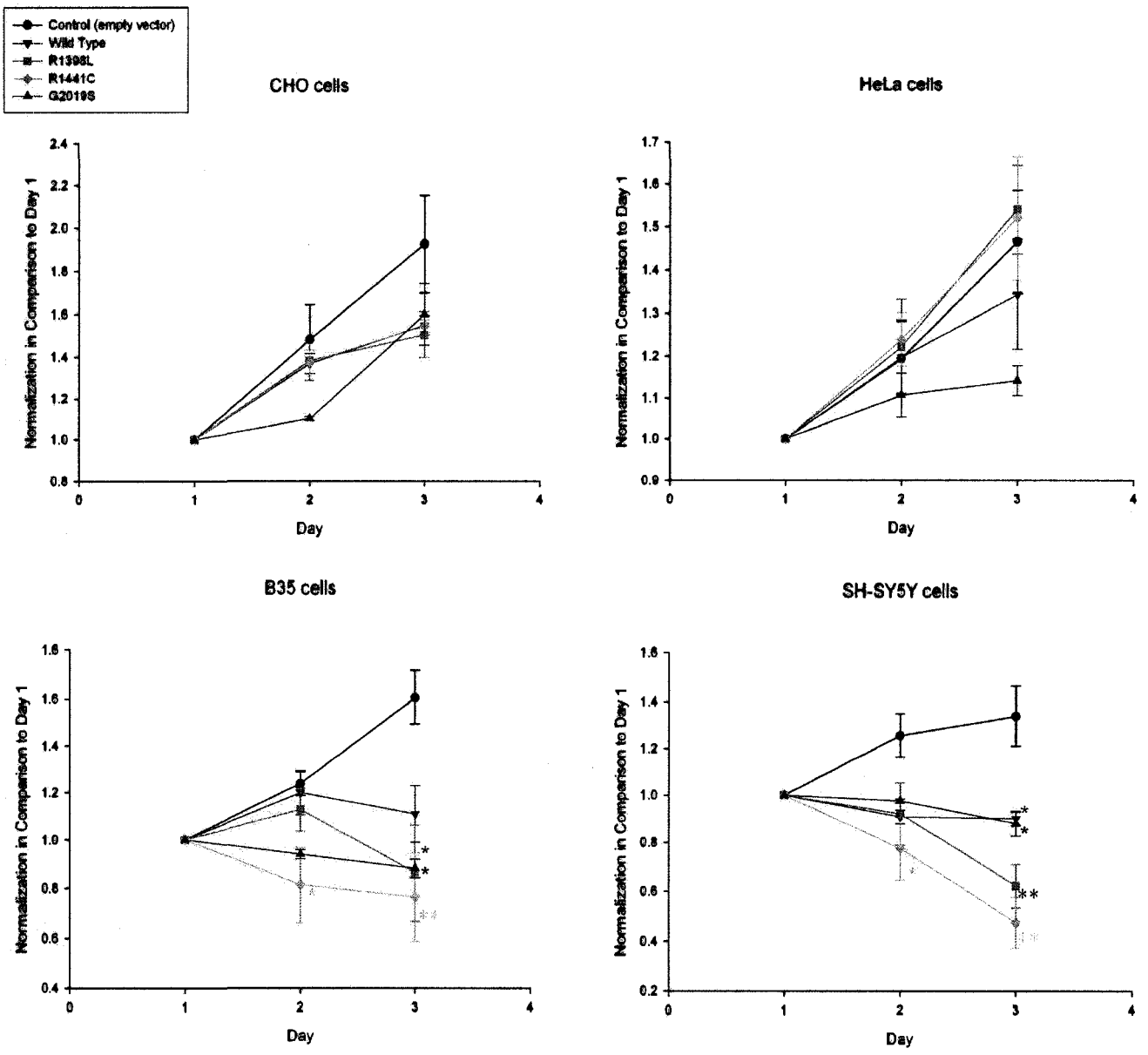

Figure 6: LRRK2 Overexpression leads to neuronal cell degeneration
Trypan blue cell death assay illustrates that overexpression of LRRK2 leads to a decrease in cell survival over time in neuronal-like cell lines (B35 and SH-SY5Y), but not in fibroblast-like cell lines (CHO and HeLa). Cells were co-transfected with pcDNA3.1(+) LRRK2 constructs and pEGFP and counted over 3 days to determine the survival rate of the cells. As a positive control to make sure no other factors (i.e. transfection reagent, cell media) were interfering with cell growth, pEGFP was co-transfected with the empty pcDNA3.1(+) myc vector and scored for survival in parallel to the LRRK2 constructs (*$p<0.05$, **$p<0.001$).

LRRK2 often has a punctate morphology within the cytoplasm

Confocal microscopy was used to determine the subcellular localization of myc-tagged LRRK2 wild type, Rab mutant, and kinase G2019S mutant constructs transiently transfected in CHO cells. All four constructs most often seemed to have punctate staining throughout the cytoplasm (Figure 7Ai), which was compared to different subcellular structures to determine if LRRK2 could be associated with them. After fixation, cells were co-immunolabelled with antibodies specific for distinct subcellular structures.

It was of interest to determine which intracellular organelles could be associated with the punctate structures identified with LRRK2 staining. Therefore co-localization analysis was used to determine whether LRRK2 associated with different structures using various markers to identify them: Mannosidase II for the Golgi complex, EEA1 for early endosomes, and calreticulin for the endoplasmic reticulum (ER). There was no overlap that could be confirmed with the Golgi apparatus (Figure 8) or early endosomes (Figure 9), and very slight, co-localization with the ER (Figure 10), suggesting that the punctate structures are either related to, or derived from the ER.

Through subcellular fractionation, 10% of the LRRK2 protein was shown by West and colleagues [42] to localize to the mitochondria. Therefore this structure was also stained in LRRK2 transfected cells to see if the protein could be detected in the same area as the mitochondria (anti-cytochrome c), but this was also not conclusive (Figure 11).

LRRK2 R1441C mutant has a 'cage-like' phenotype in 35 % of transfected cells

Although LRRK2 has a punctate morphology, the R1441C mutant construct was interesting because it showed a 'cage–like,' filamentous structure around the nucleus in about 35% of transfected cells (Figure 7Aii). As a result, LRRK2 transfected cells were scored for this morphology in all constructs being studied to determine whether or not the differences between groups were important (Figure 7B). When all groups were evaluated, it was found that there was no striking difference in morphology when comparing the wild type, R1398L, and G2019S constructs. More than 98% of cells had the usual, cytosolic, punctate staining. However when these groups were compared to the R1441C mutant which had only 65% cells with the usual morphology, there was a significant difference ($p < 0.001$), indicating that this phenotype was specific to this mutant (Figure 7B).

This unusual morphology was then compared with other structures in the cell to determine if there was any association with specific cell structures. Cells were therefore stained for the microtubules (anti-alpha tubulin, anti-acetylated tubulin) and intermediate filaments (anti-vimentin) to determine if there was any co-localization with these structures. There was partial co-localization of these filamentous structures with vimentin (intermediate filament marker) as seen in Figure 12, as well as with the microtubules (Figures 13 and 14). Full co-localization however, could not be confirmed with either of these structures. The usual punctate staining did not seem to co-localize with the intermediate filaments but the microtubules had partial co-localization.

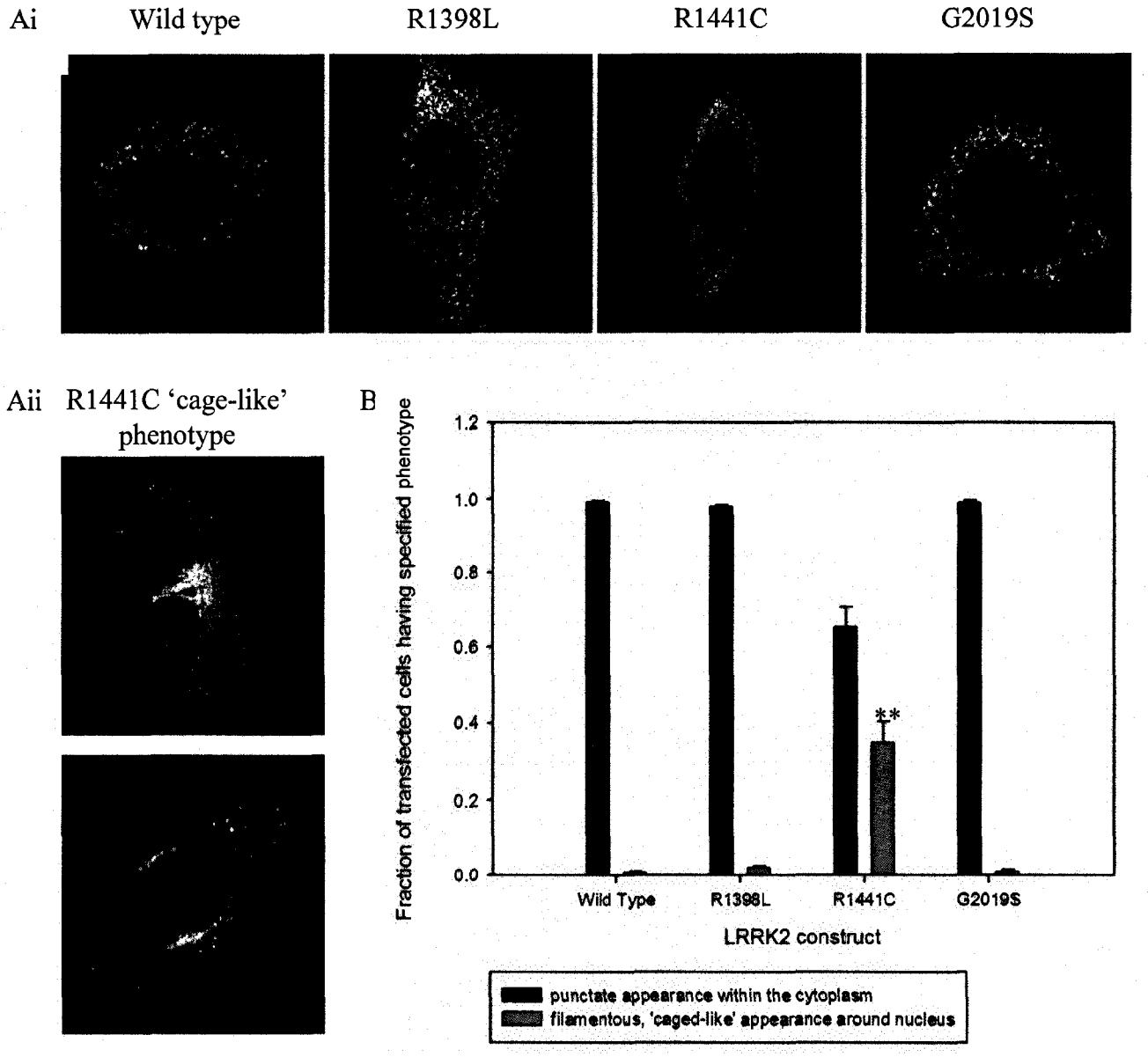

Figure 7: LRRK2 protein expression pattern in CHO cells.
LRRK2 transfected cells usually show a punctate pattern within the cytosol, but a fair percentage of the R1441C construct also seems to align with filamentous structures in the cell.

A. CHO cells were transiently transfected with pcDNA3.1(+) myc LRRK2 wild type and mutant constructs. After 48 hours, cells were fixed and stained with mouse anti myc antibody to detect the protein.
   i. Top panel shows usual punctate phenotype of LRRK2 transfected cells
   ii. Lower panels represent the R1441C mutant filamentous phenotype observed.

B. Cells were scored to determine the amount of cells in each construct having the filamentous phenotype seen in the R1441C mutant and compared statistically using the ANOVA followed by the Tukey-Kramer post hoc test. The dark blue column represents cells having the usual punctate phenotype, while the light blue column represents cells with the filamentous phenotype (** represent $p<0.001$).

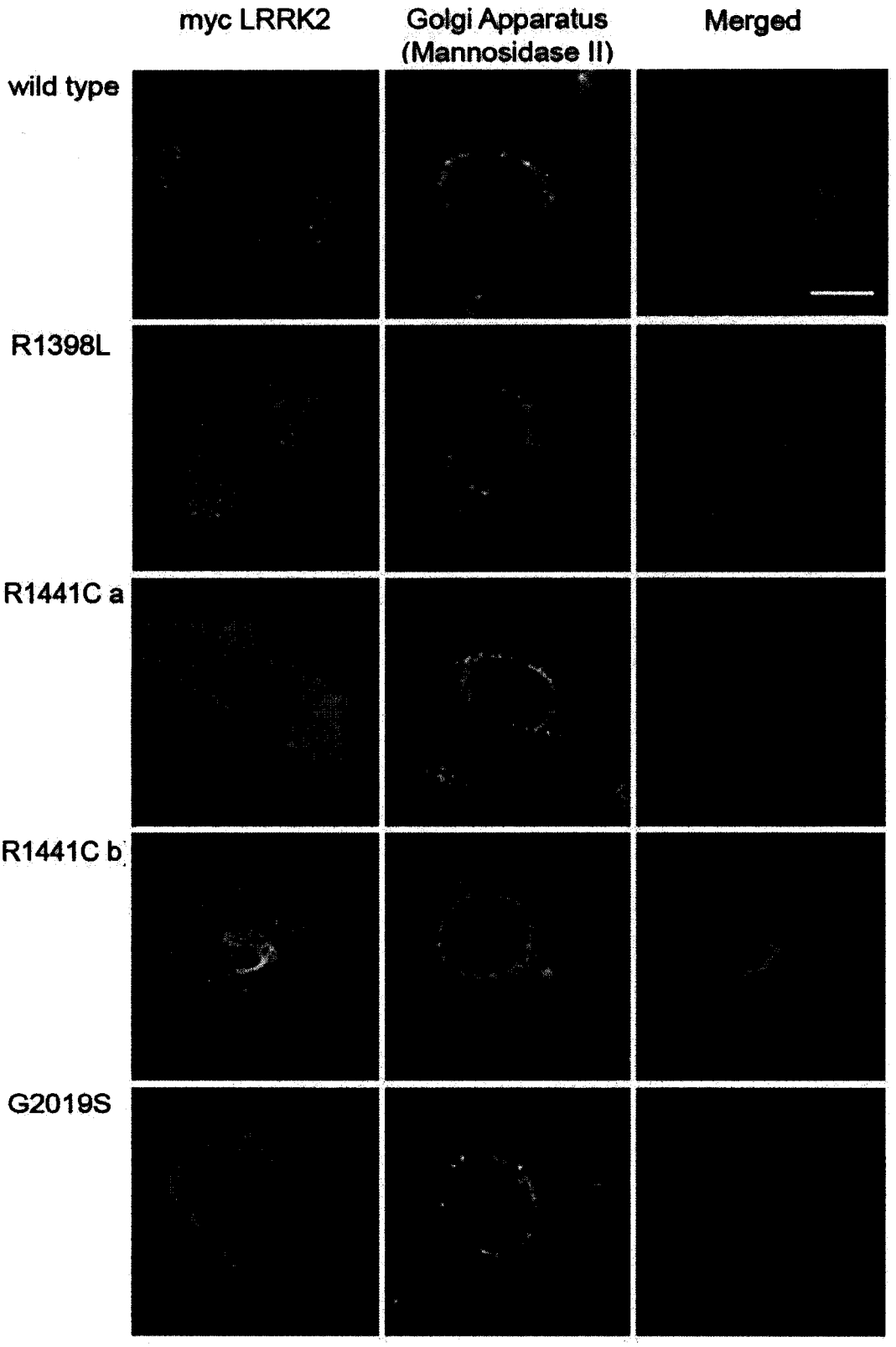

Figure 8: Immunocytochemical analysis of LRRK2 in comparison to the Golgi apparatus. Immunofluorescence to detect any co-localization of myc-tagged LRRK2 with Mannosidase II (Mann II), which labels the Golgi apparatus. CHO cells were transfected with myc-tagged wild type or mutant LRRK2 constructs. The cells were stained with mouse monoclonal anti-myc together with rabbit polyclonal anti-Mannosidase II. Two panels --R1441C a) and R1441c b) – were created to compare both the punctate and filamentous morphologies observed in this mutant to the Golgi. The merged image shows the myc LRRK2 signal in green and the Mann II signal in red. No co-localization could be confirmed (White scale bar in top right hand panel is equal to 10 microns.).

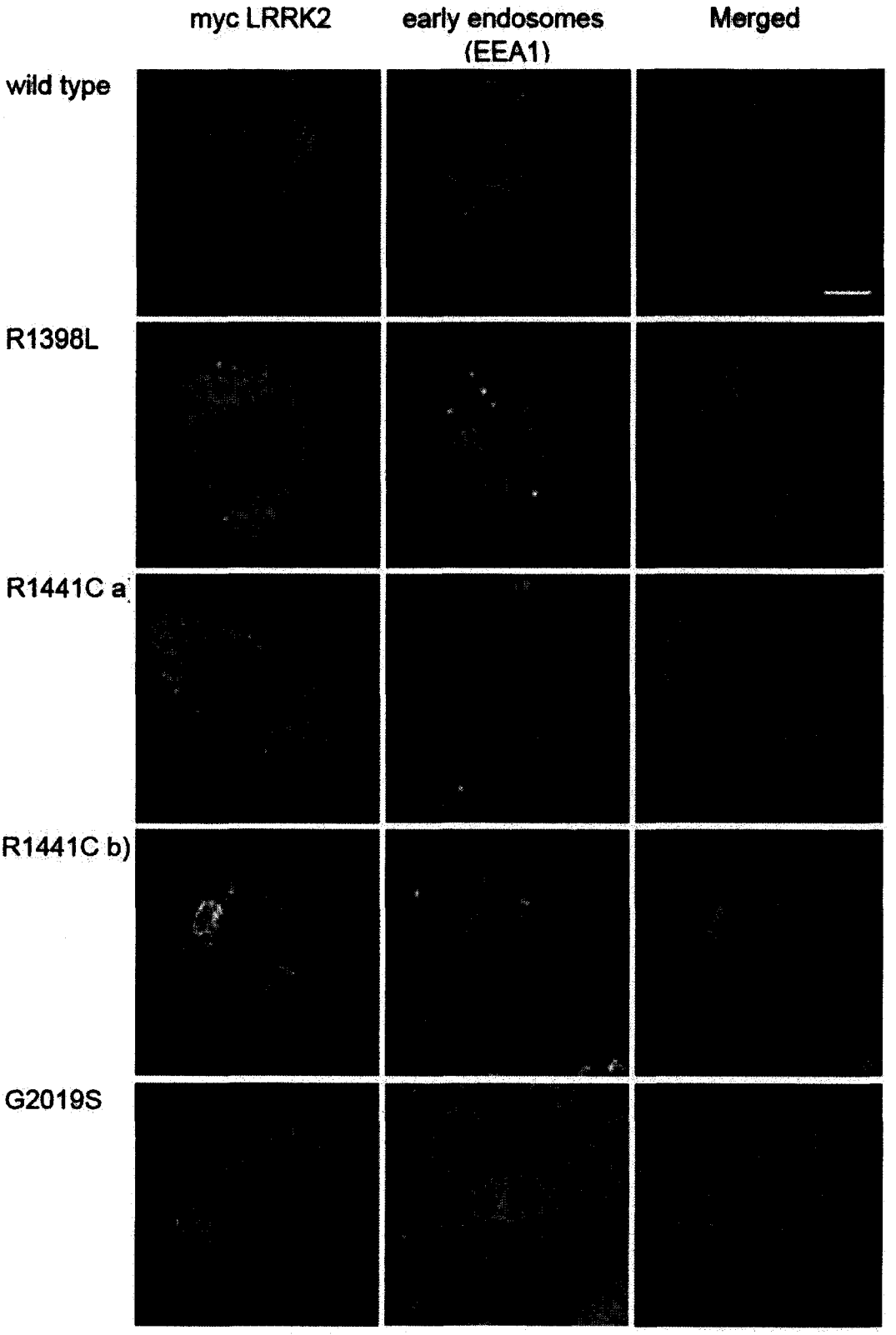

Figure 9: Immunocytochemical analysis of LRRK2 in comparison to the early endosomes. CHO cells were transfected with myc-tagged wild type or mutant LRRK2 constructs. The cells were stained with mouse monoclonal anti-myc to detect LRRK2 and rabbit polyclonal anti-EEA1 to label the early endosomes. Two panels -- R1441C a) and R1441c b) – were created to compare both the punctate and filamentous morphologies observed in this mutant to the early endosomes. The merged image shows the myc LRRK2 signal in green and the EEA1 (early endosome) signal in red. No co-localization could be confirmed. (White scale bar in top right hand panel is equal to 10 microns.)

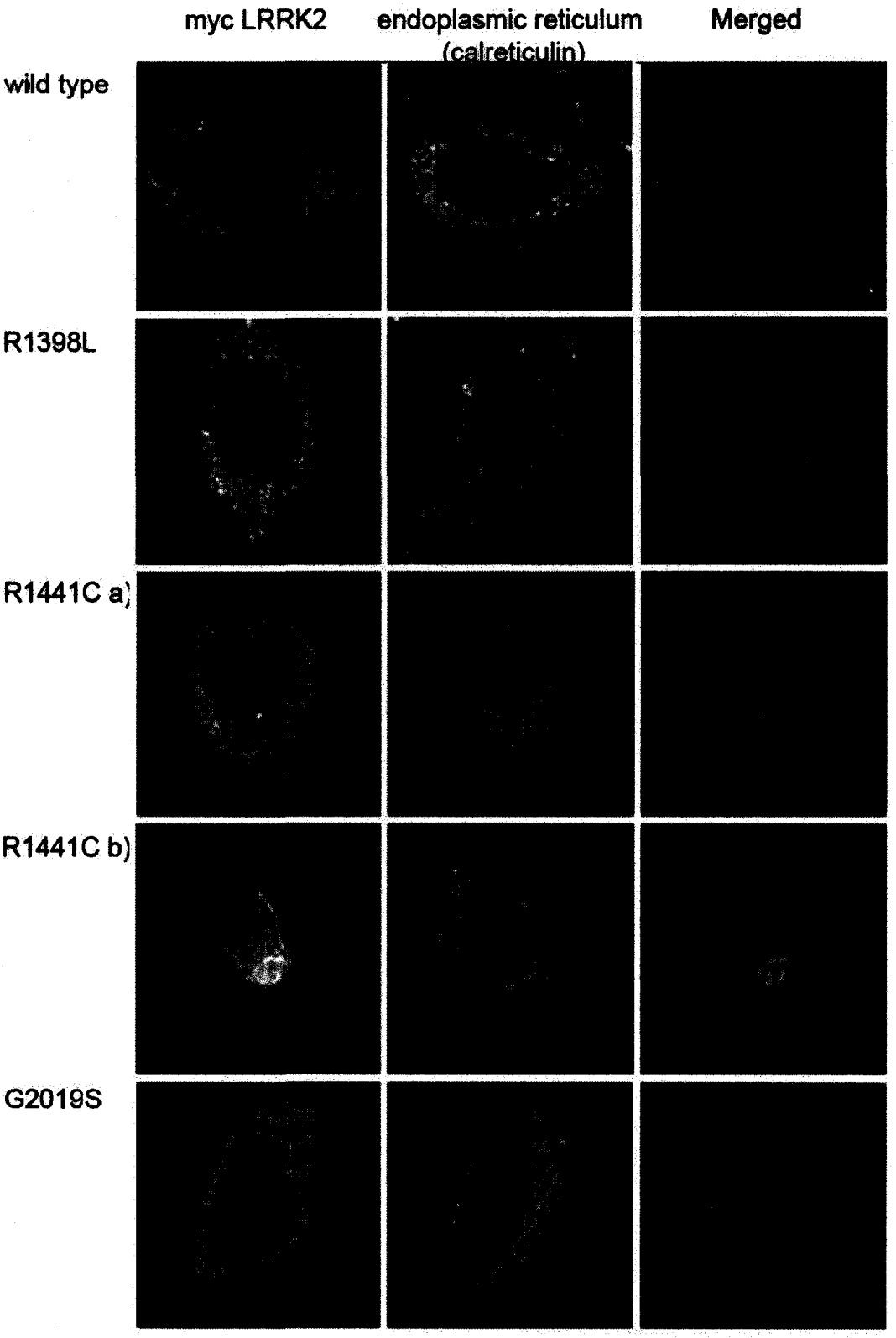

Figure 10: Immunocytochemical analysis of LRRK2 in comparison to the ER.
CHO cells were transfected with myc-tagged wild type or mutant LRRK2 constructs. The cells were stained with mouse monoclonal anti-myc to detect LRRK2 and rabbit polyclonal anti-calreticulin to detect the ER. Two panels --R1441C a) and R1441c b) – were created to compare both the punctate and filamentous morphologies observed in this mutant to the ER. The merged image shows the myc LRRK2 signal in green and the calreticulin (ER) signal in red. Very slight co-localization could be observed with the punctate LRRK2 staining (yellow dots in merged image) (White scale bar in top right hand panel is equal to 10 microns.).

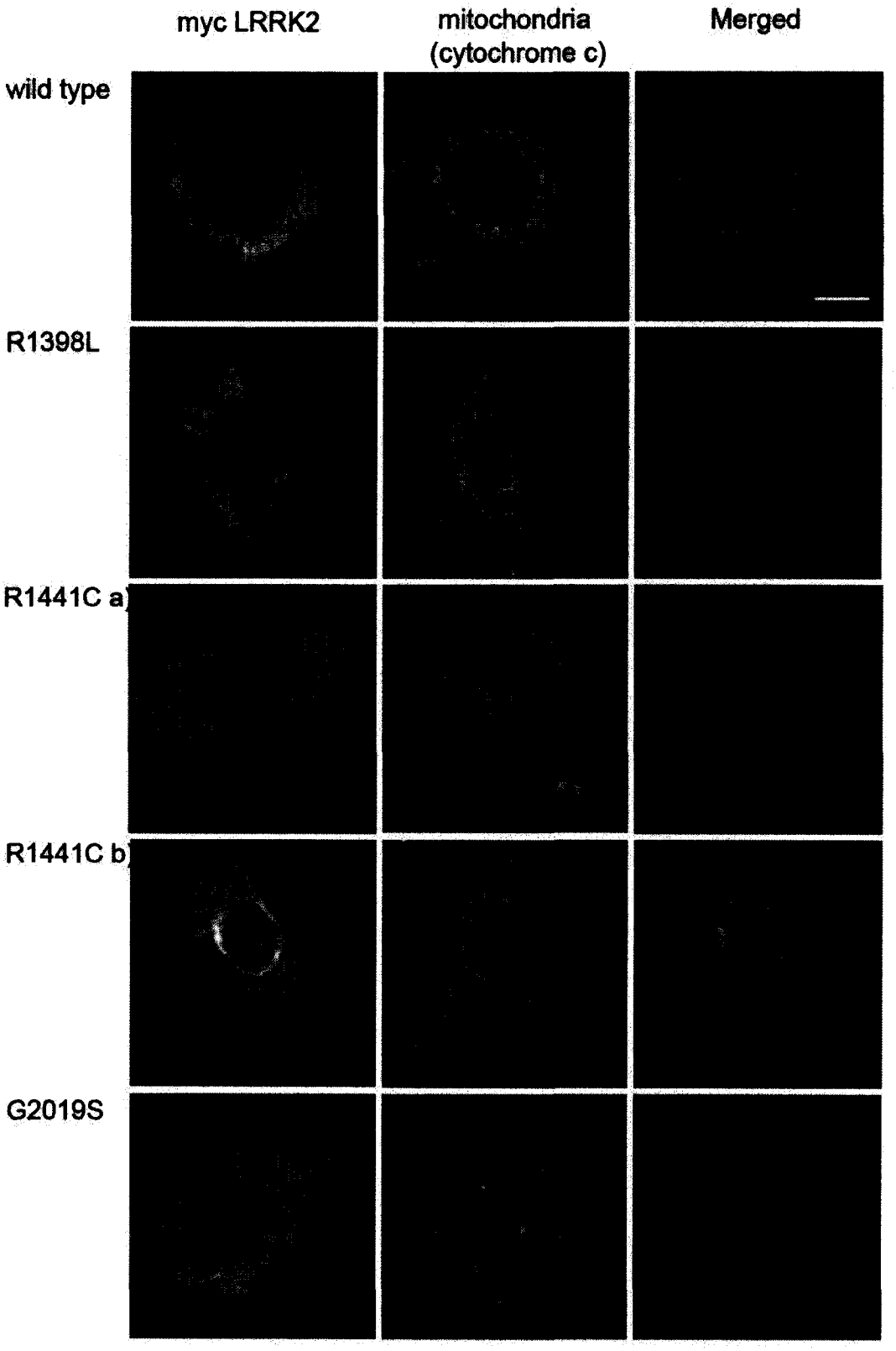

Figure 11: Immunocytochemical analysis of LRRK2 in comparison to the mitochondria. CHO cells were transfected with myc-tagged wild type or mutant LRRK2 constructs. The cells were stained with rabbit polyclonal anti-myc to detect LRRK2 and mouse monoclonal anti-cytochrome c to visualise the mitochondria. Two panels --R1441C a) and R1441c b) – were created to compare both the punctate and filamentous morphologies observed in this mutant to the mitochondria. The merged image shows the myc LRRK2 signal in green and the cytochrome c (mitochondrial) signal in red. No co-localization could be confirmed (White scale bar in top right hand panel is equal to 10 microns).

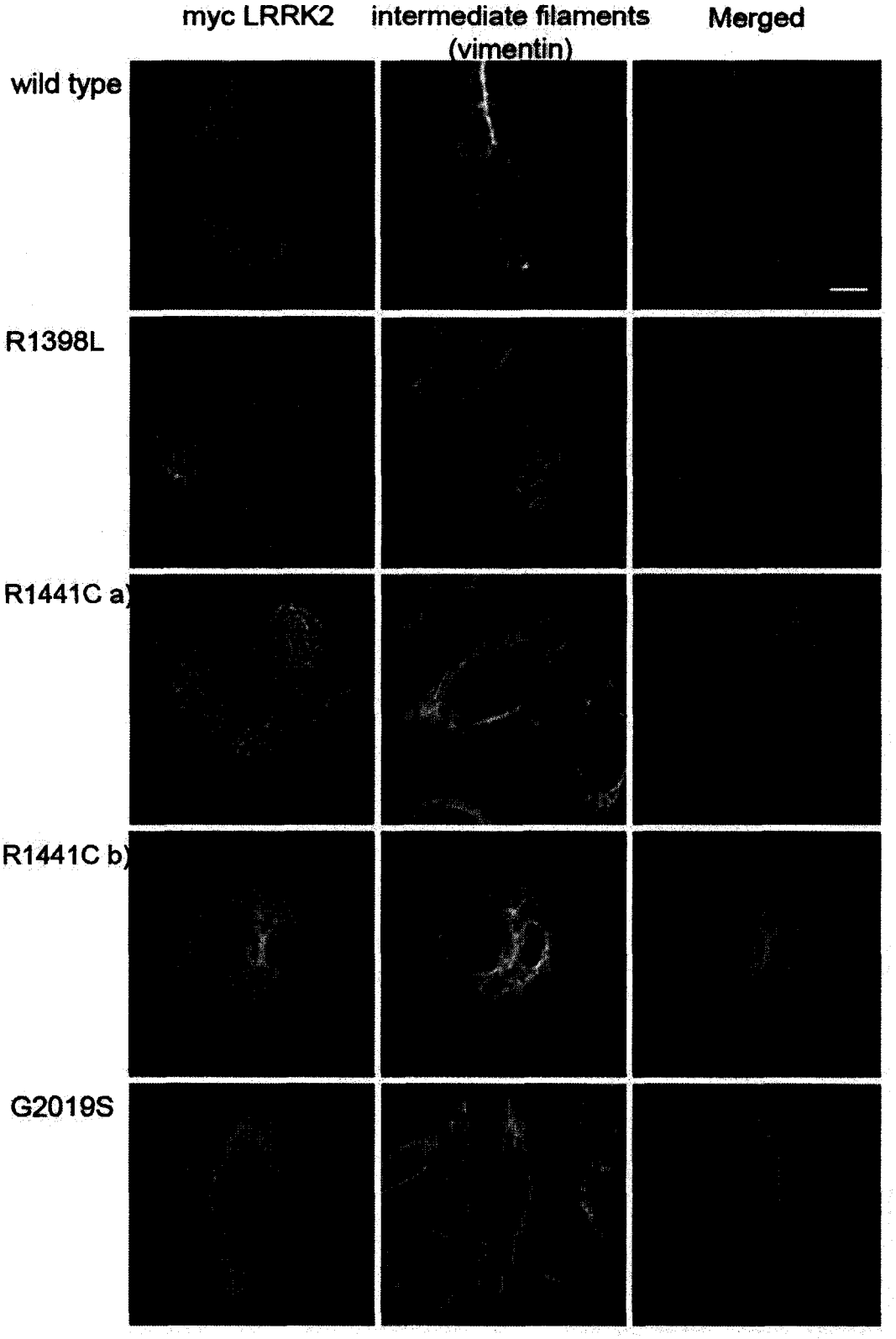

Figure 12: Immunocytochemical analysis of LRRK2 in comparison to the intermediate filaments. CHO cells were transfected with myc-tagged wild type or mutant LRRK2 constructs. The cells were stained with rabbit polyclonal anti-myc to detect LRRK2 and mouse monoclonal vimentin to label the intermediate filament structures. Two panels --R1441C a) and R1441c b) – were created to compare both the punctate and filamentous morphologies observed in this mutant to these structures. The merged image shows the myc LRRK2 signal in green and the intermediate filament signal in red. There seems to be some co-localisation in the R1441c b) panel showing the filamentous phenotype, but not in any other panels. (White scale bar in top right hand panel is equal to 10 microns.)

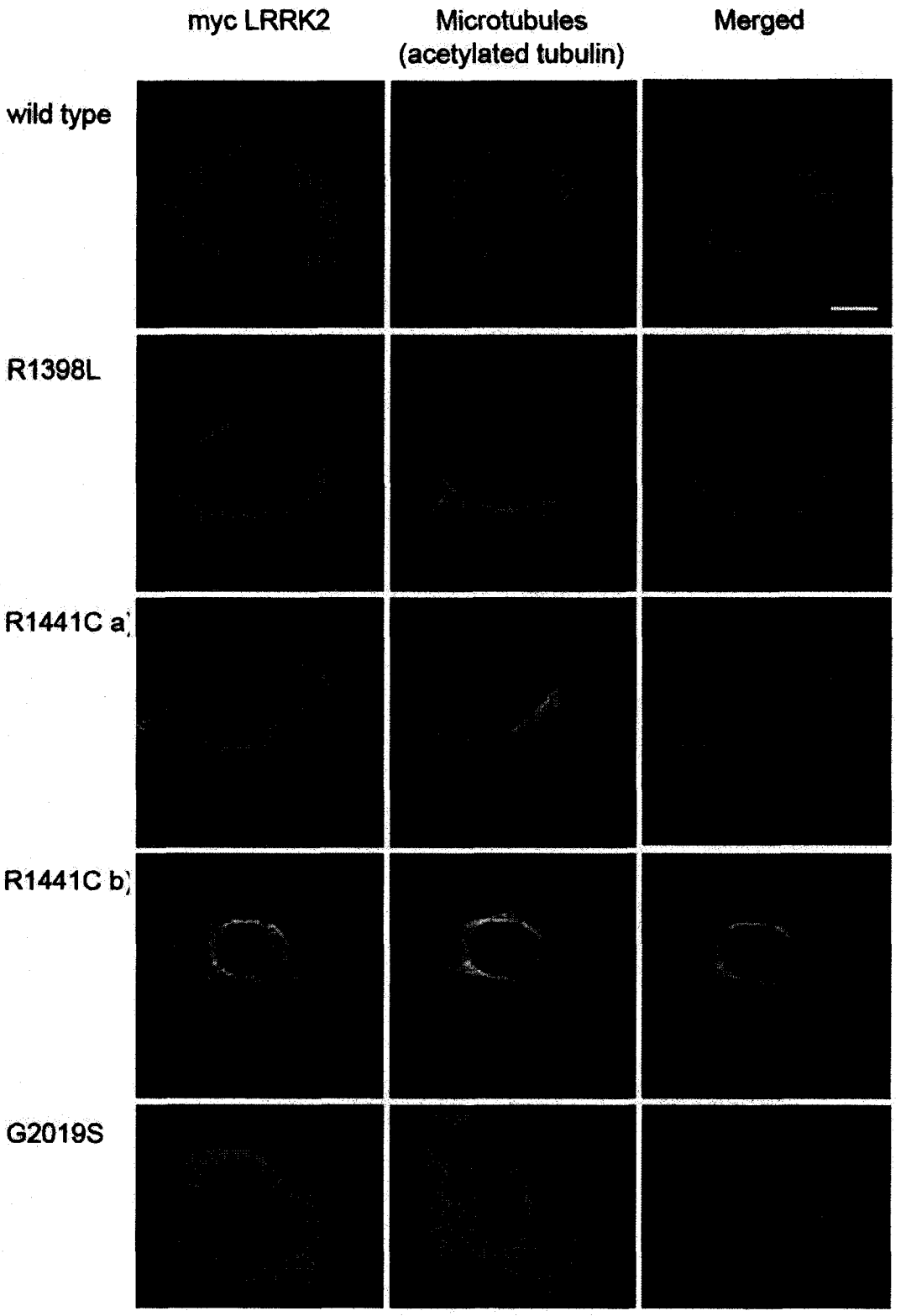

Figure 13: Immunocytochemical analysis of LRRK2 in comparison to the microtubules (acetylated).CHO cells were transfected with myc-tagged wild type or mutant LRRK2 constructs. After 48 hours, the cells were fixed and stained with rabbit polyclonal anti-myc to detect LRRK2 and mouse monoclonal anti-acetylated tubulin, a microtubule marker. Two panels --R1441C a) and R1441c b) – were created to compare both morphologies observed in this mutant to these structures. The merged image shows the myc LRRK2 signal in green and the microtubule signal in red. There seems to be some co-localisation in the R1441c b) panel showing the filamentous phenotype, but not much co-localization in the other panels (White scale bar in top right hand panel represents 10 microns.)

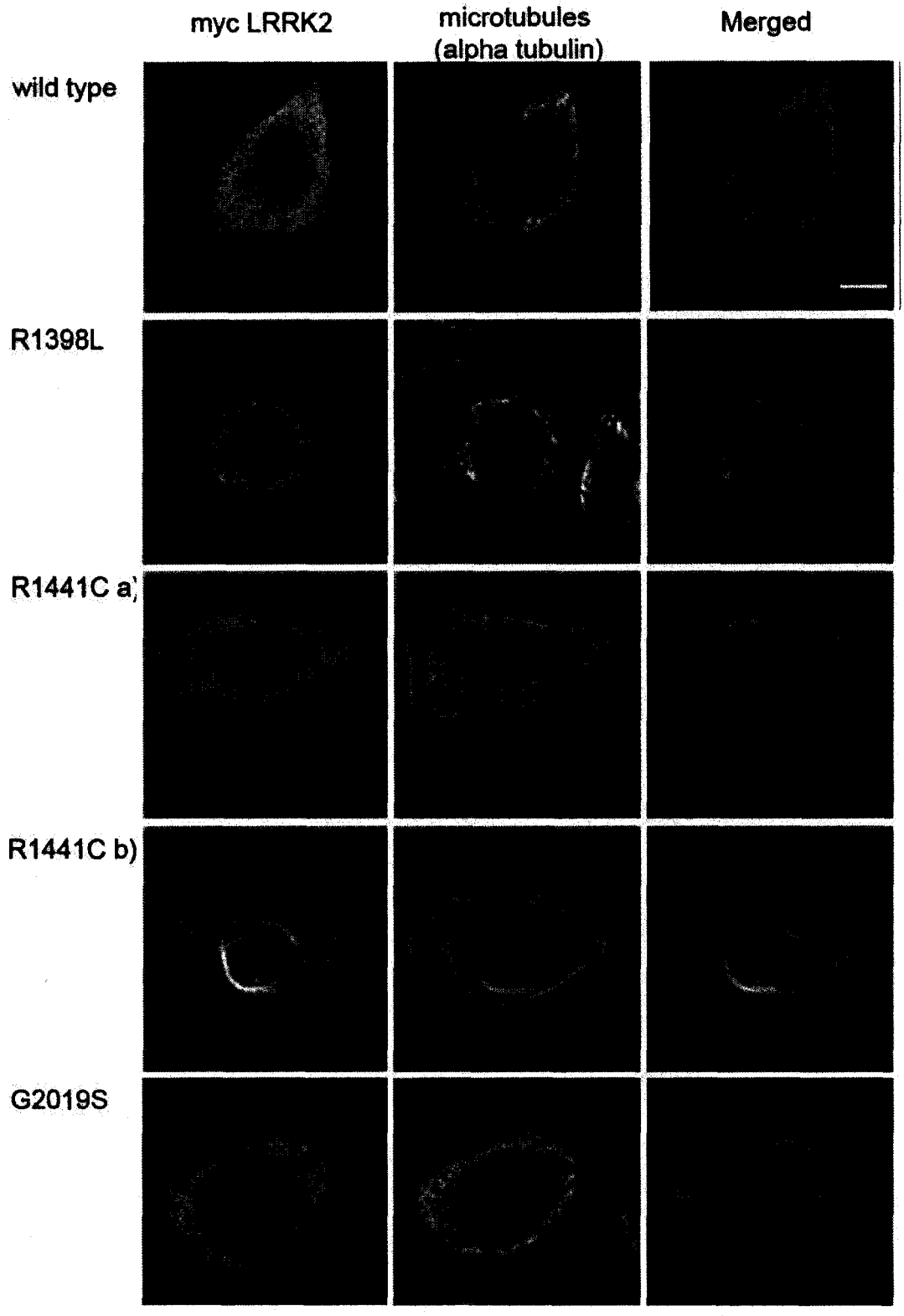

Figure 14: Immunocytochemical analysis of LRRK2 in comparison to the microtubules. CHO cells were transfected with myc-tagged wild type or mutant LRRK2 constructs. After 48 hours, the cells were fixed and stained with rabbit polyclonal anti-myc to detect LRRK2 and mouse monoclonal anti-alpha tubulin, a microtubule marker. Two panels --R1441C a) and R1441c b) – were created to compare both morphologies observed in this mutant to these structures. The merged image shows the myc LRRK2 signal in green and the microtubule signal in red. There seems to be some co-localisation in the R1441c b) panel showing the filamentous phenotype, and slight co-localization in the other panels as well (White scale bar in top right hand panel represents 10 microns.).

The data suggests that LRRK2 is a cytoplasmic protein possibly associated with the endoplasmic reticulum, microtubules, and intermediate filaments. The R1441C mutant construct seems to disrupt the usual morphology of LRRK2 resulting in filamentous 'cage-like' structures around the nucleus.

LRRK2 may be associated with microtubule network

There was slight co-localization of these 'cage-like' structures in the R1441C mutant with vimentin. Depolymerisation of the microtubules of LRRK2 transfected cells with colchicine, and its impact on the intermediate filaments became intriguing to study.

The cytoskeleton of the cell is made up of three types of fibers -- microtubules, microfilaments and intermediate filaments -- to help maintain the structure and organization of the cell. Vimentin intermediate filaments have been associated with the microtubules, as a physical linkage between these fibers has been detected with drugs. Treatment of cells with 1 μg/ml colchicine for 24 hours caused the complete dissolution of microtubules, and although vimentin filaments remained intact, they clumped into disorganized bundles toward the nucleus. The organization of vimentin filaments is therefore, dependent on intact microtubule structure.

Cells transfected with LRRK2 wild type and mutant Rab constructs were treated with 1 μg/ml colchicine for 24 hours (Figure 15: test assay). Colchicine works to depolymerize the microtubules by binding to tubulin. The vimentin staining pattern in both transfected and untransfected cells seemed more disorganized and clustered, while the microtubules were completely depolymerized (punctate staining pattern with alpha tubulin). The LRRK2 staining pattern was cytoplasmic and punctate for all three LRRK2 constructs. What was especially surprising to note was that the 'cage-like' filaments in

the R1441C construct had disappeared (Colchicine treatment, Figure 16). Thus, there may be a link between the microtubules and LRRK2.

Microtubules (alpha tubulin)

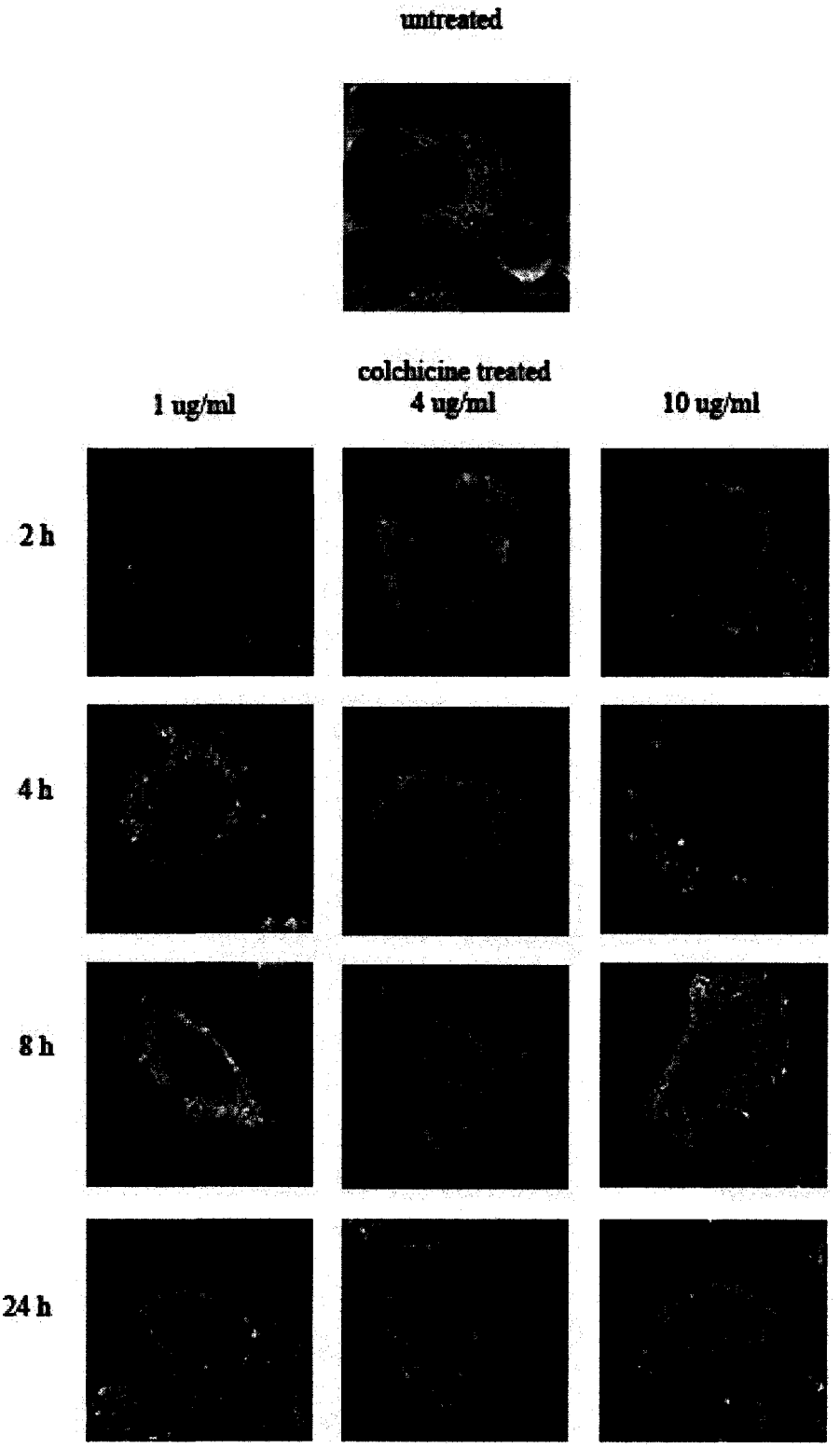

Figure 15: Colchicine test assay in CHO cells.

A. *Immunofluorescence to detect depolymerisation of the microtubules after treatment with colchicine.* CHO cells were treated with varying concentrations of colchicine for different periods of time, while one set of cells was left untreated to view as a control. The cells were stained with mouse monoclonal anti-alpha tubulin to make sure the microtubules were depolymerised. 1ug/ml colchicine after 2 hours is enough to cause depolymerisation (punctate staining in comparison to long filaments in control). White scale bar in top panel represents 10 microns.

Intermediate Filaments (vimentin)

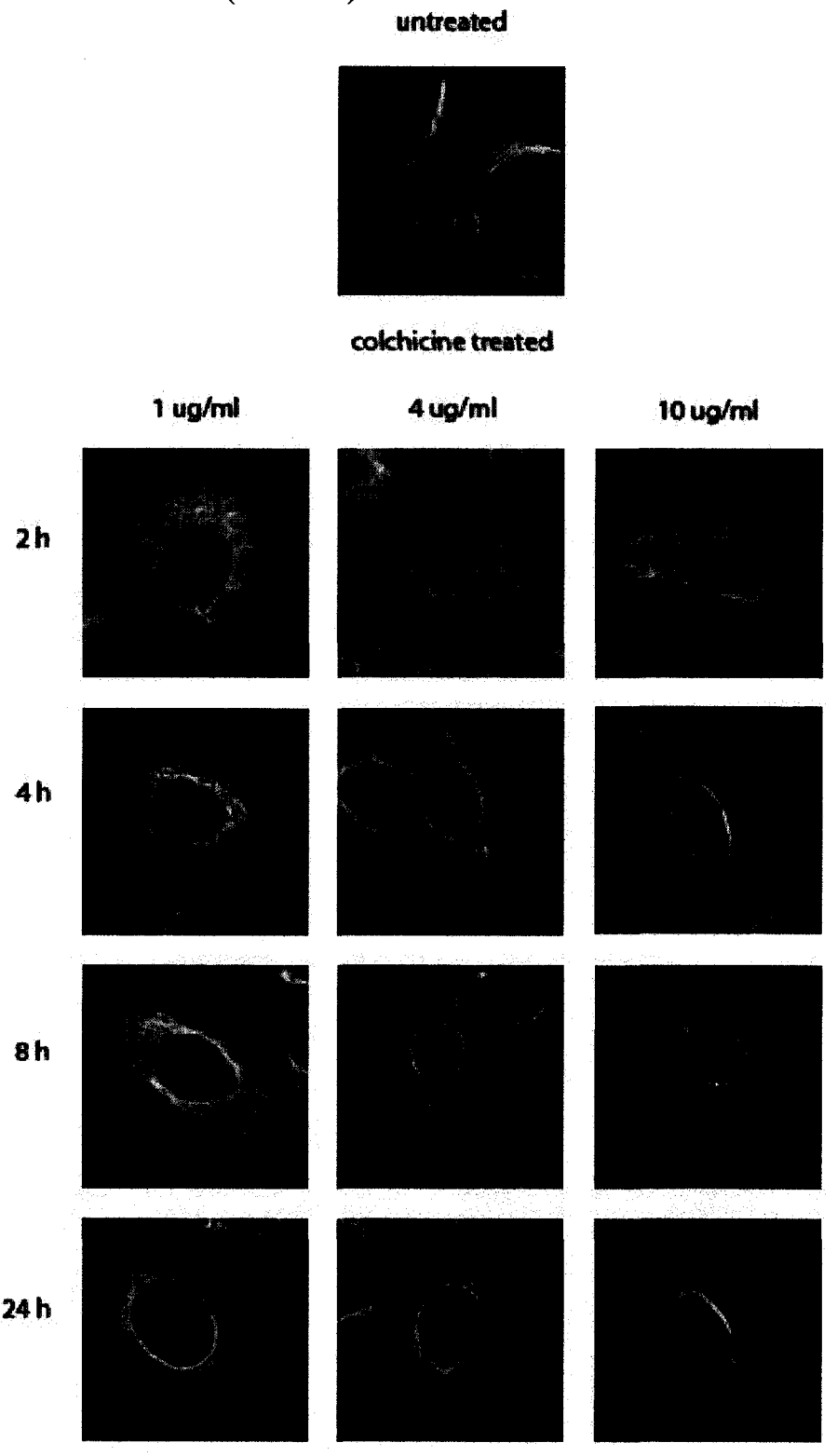

Figure 15: Colchicine test assay in CHO cells.

B. *Immunofluorescence to detect changes in the structure of the intermediate filaments after treatment with colchicine.* CHO cells were treated with varying concentrations of colchicine for different periods of time, while one set of cells was left untreated to view as a control. The cells were stained with mouse monoclonal anti-vimentin to look for changes in the intermediate filaments. It can be seen even with 1ug/ml after 24 hours, that these structures have collapsed inward, and are not branched out as normally seen in the control. White scale bar in top panel represents 10 microns.

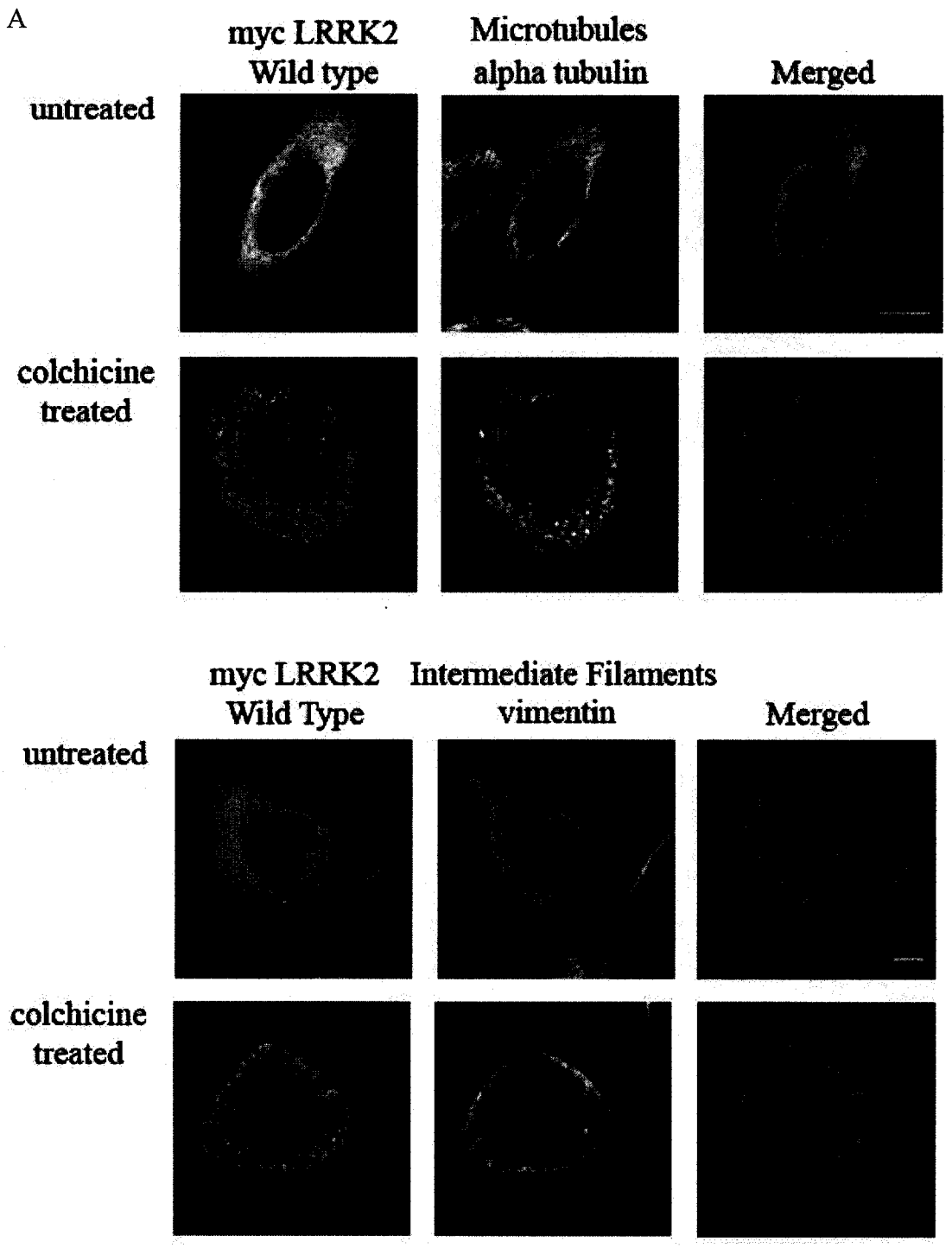

Figure 16: Colchicine treatment of LRRK2 Transfected Cells.

A. *Immunofluorescence to detect LRRK2 wild type morphology, depolymerisation of the microtubules, and changes in the structure of the intermediate filaments.*

CHO cells were transfected with myc-tagged wild-type LRRK2 constructs. One set of cells was treated with colchicine while the other set was untreated as a control. The cells were stained with rabbit polyclonal anti-myc together with rabbit mouse monoclonal anti-alpha tubulin in the top panels showing microtubule depolymerisation. The bottom panels show that the intermediate filaments are collapsed after colchicine treatment with no major change in the usual punctuate morphology of LRRK2.

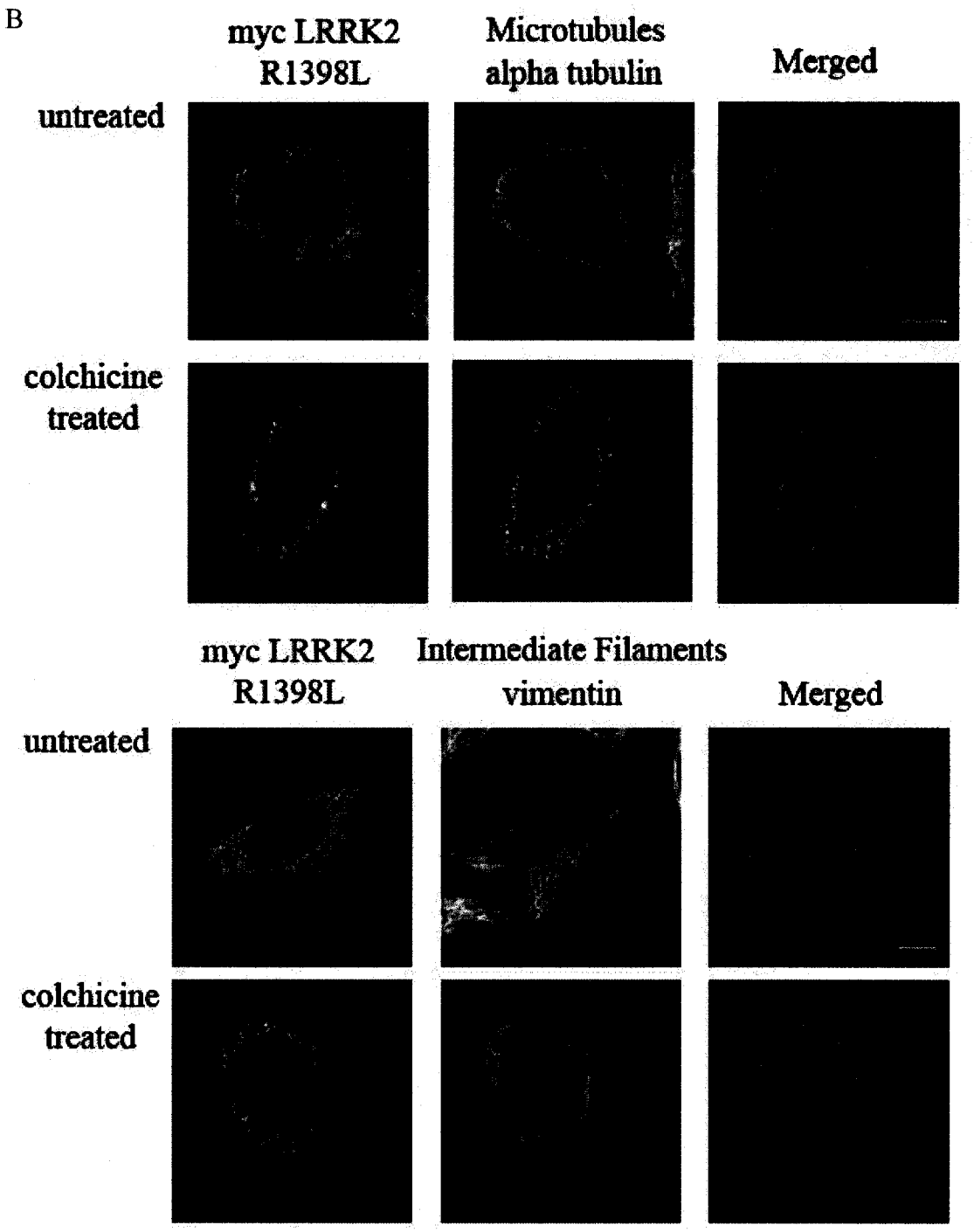

Figure 16: Colchicine treatment of LRRK2 Transfected Cells.

B. *Immunofluorescence to detect LRRK2 R1398L morphology, depolymerisation of the microtubules, and changes in the structure of the intermediate filaments.*

Cells were transfected with myc-tagged LRRK2 R1398L constructs. One set of cells was colchicine treated while the other set was untreated as a control. The cells were stained with rabbit polyclonal anti-myc to detect LRRK2, together with mouse monoclonal anti-alpha tubulin in the top panels showing microtubule depolymerisation. The bottom panels show that the intermediate filaments (monoclonal anti-vimentin) are collapsed after colchicine treatment, with no major change in the usual punctuate morphology of LRRK2.

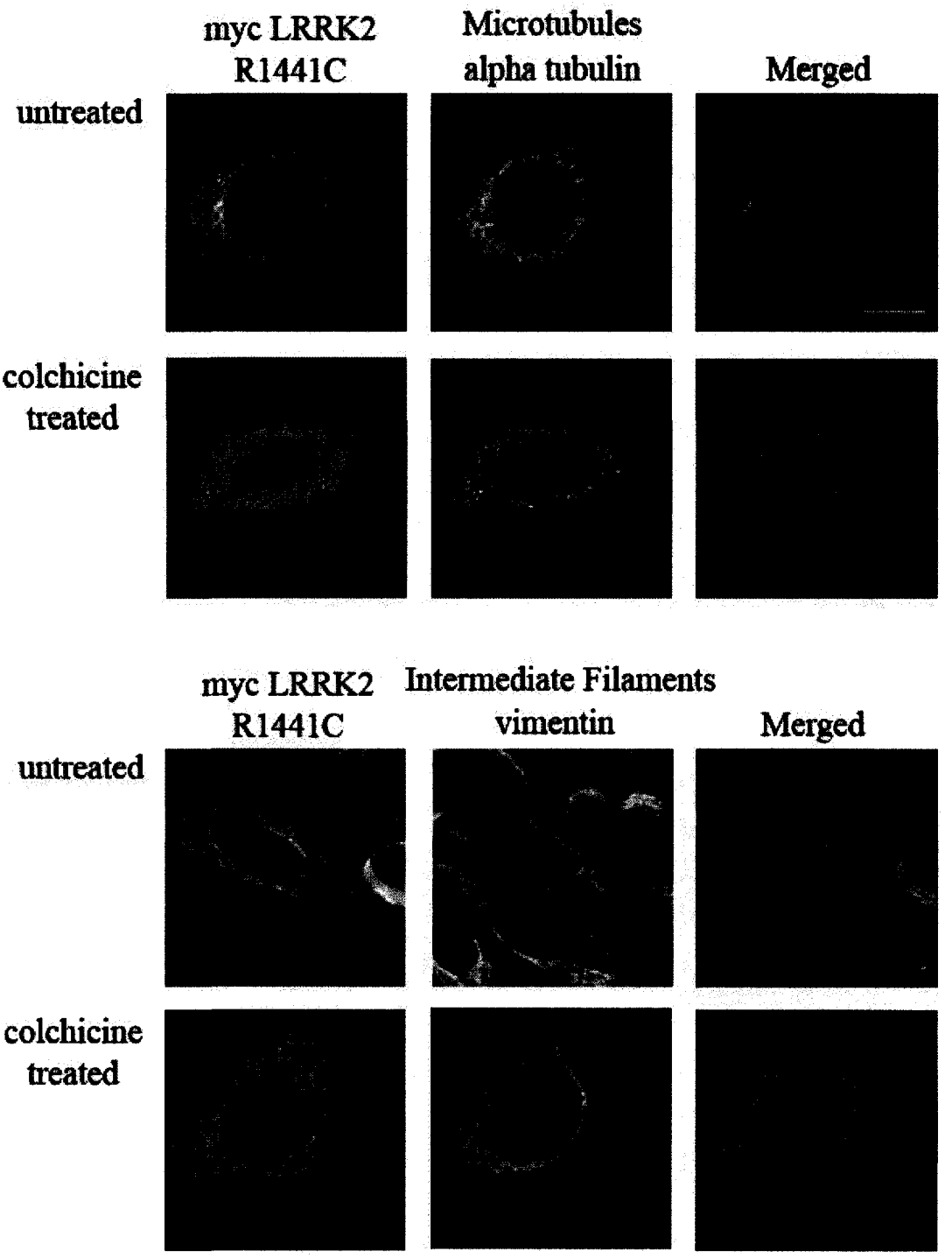

Figure 16: Colchicine treatment of LRRK2 Transfected Cells.

C. *Immunofluorescence to detect LRRK2 R1441C morphology, depolymerisation of the microtubules, and changes in the structure of the intermediate filaments.*

CHO cells transfected with myc-tagged R1441C LRRK2 constructs were treated with colchicine while another set was left untreated as a control. The cells were stained with rabbit polyclonal anti-myc to detect LRRK2, together with mouse monoclonal anti-alpha tubulin in the top panels showing microtubule depolymerisation. The bottom panels show that the intermediate filaments (monoclonal anti-vimentin) are collapsed after colchicine treatment. The unusual filamentous morphology seen in one-third of untreated cells was not apparent after treatment.

DISCUSSION

Rab domain mutations within the LRRK2 protein disrupt intrinsic GTP hydrolysis rate.

Rab proteins are small GTPases that act as molecular switches regulating different processes in the cell through cycling GTP (active) for GDP (inactive). In LRRK2, the Roc domain bares resemblance to Rab proteins when considering the subfamilies in the Ras protein superfamily [20]. Therefore, the Rab domain of LRRK2 was tested for GTP hydrolysis by recording inorganic phosphate release. The wild type Rab domain protein of LRRK2, along with two different Rab domain constructs with the following mutations were purified: R1441C, which is associated with PD, and R1398L, which according to sequence homology should make the Rab domain active site constitutively active. There was a slow rate of hydrolysis in the wild type construct, but the mutants were even slower to hydrolyze GTP (Figure 4). Other groups had found that LRRK2 was able to bind GTP, and therefore focus was directly concentrated on the hydrolysis assay to see if LRRK2 could hydrolyze GTP. However, this assay would have been more reliable if GTP binding was first confirmed by these constructs, without necessarily relying on the data of others.

When compared to the studies previously completed on LRRK2 hydrolysis, this study adds evidence that LRRK2 does have GTPase activity. The differences in GTP hydrolysis rates among constructs could be accounted for in the R1398L mutant, because this mutation, through sequence homology was shown to make the Roc domain constitutively active by interfering with the gamma phosphate binding site thereby preventing GTP hydrolysis. When directly compared to Ras, the R1398 position in

LRRK2 corresponds to the Q61 position in Ras which is essential in interacting with the gamma-phosphate of the GTP substrate [51]. As a result of this interference, the domain would be unable to hydrolyze GTP.

The R1441C mutation is not in the GTP binding site, but resides far away from the catalytic site, on the surface of the Rab domain, thereby probably interfering with protein binding. This pathogenic mutation is located within the Roc domain on the end of alpha helix 3 which interacts with alpha helix 2 at the dimer interface [51]. The arginine residue is important in stabilizing interactions on the dimer surface as the guanidium group forms hydrogen bonds with backbone residues to help, as previously mentioned, in the formation of "alternating stacks to produce a hydrophobic 'greasy' zipper across the dimer interface" [51]. Loss of this stabilization due to arginine substitutions being replaced by shorter side chains such as cysteine, could result in the displacement of two key residues, R1398 and D1394, needed to interact with the gamma-phosphate of GTP and Mg^{+2} ion. Therefore, the instability of dimer formation could lead to the low levels of GTP hydrolysis observed through the GTPase assay.

LRRK2 has been found by different research groups [33, 64] to exist as a dimer. Although groups have found a few other Rab proteins with crystal structures as dimers, they also mention that the proteins would probably exist in this state during periods favoring low affinity interactions [65, 66] because at physiological conditions, or in solution, the proteins have been found as monomers. Most Rab proteins identified to date are not known to exist in this form. Of other small GTPases however, some studies have shown that Ras must form a dimer upon entering the plasma membrane in order to activate it's substrate, Raf1 [67]. There is also evidence that Rho proteins, including

RhoA, Rac2, and Cdc42, undergo dimerization when bound to GTP through interactions with their polybasic C-terminal domain which have yet to be identified. Both Rac2 and Cdc42 have shown intrinsically higher GTP hydrolysis rates as a dimer, comparable to the activity of the monomer bound to its GAP [68].

Dimerization of the Roc domain in LRRK2 may help stabilize protein interactions within LRRK2 in the active state, like Rho proteins, which may assist in providing negative regulation of the kinase domain by increased GTP hydrolysis. Research by Guo et al [53] suggested that the rate of hydrolysis of the LRRK2 Roc domain was comparable to that of the Rho protein, Rac1. It should be noted though, that the LRRK2 Roc has been predominantly found in the dimer form when bound to both GDP and GTP, unlike the Rho proteins which seem to form the dimer when in the active form only.

It would be interesting to compare the polybasic C-terminal domain from the Rho proteins that result in dimer formation, to the different protein interaction domains of LRRK2, especially the COR domain which was shown to interact with the Roc domain [51] to see if there is similarity in possible interactions that may lead to the formation of the Roc dimer. It also would be of interest to determine if the LRRK2 Roc monomer GTP hydrolysis rate differed from that of the dimer.

In addition to the evidence of dimerization in small GTPase proteins, there is much information pertaining to the dimerization of kinases, since many kinases exist in this state. Dimerization has a crucial role in regulation of different kinases [69]. The LRRK2 kinase domain has not been shown to contribute to the dimer complex. Instability of the dimer however, may lead to the altered rate of GTP hydrolysis observed, which

could alter kinase activity of LRRK2 thereby causing further cellular downstream activities to be unregulated.

Overexpression of the LRRK2 protein leads to neuronal cell degeneration with Rab and kinase domain mutant constructs.

As a functional kinase, LRRK2 mutations may lead to uninhibited phosphorylation activity, which could result in the cell death observed in PD. Even though LRRK2 was found to be ubiquitously expressed in different areas of the body [3], LRRK2 associated PD mutations would be expected to cause a detrimental effect on neuronal cells since this is the most affected area of PD patients.

Immunocytochemistry was conducted on neuronal-like cell lines to determine where and how the protein was expressed. The neuroblastoma cell lines, human SH-SY5Y and rat B35, were transfected with the myc-LRRK2 protein but no detectable signal could confirm any expression. Therefore, the CHO fibroblast-like cell line was eventually used to determine if LRRK2 expression could be detected in these cells, which was confirmed although at a low level.

The unsuccessful immunocytochemical results of myc LRRK2 expression in both neuronal cell lines, led to enhancing the signal by placing the LRRK2 constructs in pBUD/eGFP, and quickly purifying and concentrating the proteins to analyze through Western blot. A band just above the 250 kDa marker corresponding to the size of LRRK2 (286 kDa) (Figure 5) was observed in the CHO cells but not in the B35 cell line. The low to undetectable expression levels of LRRK2 in neuronal cell lines could be due to many reasons, including rapid protein turnover and cell death. There was evidence

however showing that overexpression of LRRK2 causes neuronal cell degeneration [41], so this was tested through a Trypan blue assay (Figure 6).

Over three days, it was found that in both fibroblast-like cell lines studied (HeLa and CHO), cells grew at a consistent rate like the control when transfected with LRRK2 constructs. However, in the neuronal-like cell lines (B35 and SH-SY5Y), the LRRK2 R1441C mutant caused significant death on Day 2. On Day 3, a striking difference in cell survival was observed in the R1398L, R1441C, and G2019S constructs when compared to the control. In addition, the SH-SY5Y cell line displayed significantly lower cell survival in the wild type transfected cells when compared to the control. This difference between the two neuronal-like cell lines could be due to species specificity of LRRK2 since the B35 cells are derived from rat, and the SH-SY5Y cells are derived form human.

The G2019S mutation was added in parallel to the other Rab constructs as it is the most prevalent mutation associated with PD today. Therefore, it was interesting to observe whether these mutants all produced the same result to determine if they were involved in the same pathway leading to PD or not. These data suggest that although all mutations seem to lead to cell death, the R1441C mutation has the most detrimental effect on cells when compared to the other mutations.

As a whole, these results lead to the assumption that LRRK2 has a more powerful effect on neuronal like cells albeit it is ubiquitously expressed in other areas of the body as well. Therefore cell context is important, as it was also shown that kinase activity of LRRK2 has a higher rate of phosphorylation in neuronal cells when compared to kidney cells [40]. Therefore there could be either a protein present in neuronal cells that is not

present in other cell types which is being activated by the LRRK2 protein, or, there could be a protein that is in other cell types which is missing in neurons that regulates LRRK2 protein kinase activity, thereby leading solely to neuronal cell degeneration. Examining the morphology of LRRK2 in CHO cells provides a better evaluated rationale to define proteins that could be interacting with LRRK2 to result in cell death.

The cellular morphology of LRRK2 most often shows punctate staining within the cytoplasm that may associate with cytoskeletal structures.

Through confocal microscopy, LRRK2 expression was detected in CHO cells, but was undetectable in the neuronal-like cell lines most probably due to the cell death that was occurring as a result of LRRK2 overexpression. All constructs most often seemed to have punctate staining throughout the cytoplasm (Figure 7Ai), consistent with other research groups who have found LRRK2 to be a cytosolic protein [33]. The usual punctate staining pattern of myc-tagged LRRK2 wild type and mutant constructs within the cytoplasm was compared to different subcellular structures to determine if LRRK2 could be associated with them through immunocytochemistry. Slight overlap was only observed with the ER (Figure 10), and could not be confirmed with the Golgi apparatus (Figure 8) or early endosomes (Figure 9), all structures involved in vesicle trafficking. LRRK2 was shown by West and colleagues [42] to localize to the mitochondria 10% of the time, but could not be confirmed in this study (Figure 11). Being associated with the ER could relate LRRK2 not only to vesicle trafficking but to cytoskeleton involvement as well. Since it has a multidomain structure, LRRK2 has the potential to be involved in such diverse functions. Although LRRK2 morphology usually appeared punctate, the R1441C mutant construct was interesting because it showed a 'cage–like,' filamentous

structure around the nucleus in about 35% of transfected cells (Figure 7Aii, B), unlike the phenotypes of the other LRRK2 constructs. These structures showed partial co-localization with vimentin (intermediate filament marker) (Figure 12) and the microtubules (Figures 13 and 14).

Overall, this data suggests that LRRK2 is a cytosolic protein associated with the ER, microtubules, and intermediate filaments, different cytoskeletal elements. The R1441C mutant construct seems to disrupt the usual morphology of LRRK2 resulting in a filamentous 'cage-like' structure around the nucleus in more than one third of transfected cells.

Three-dimensional views used to determine whether or not these filamentous structures were in the nucleus, within the nuclear envelope, or outside the nucleus, in its periphery, suggest that the structures appear outside the nucleus. However, this is not ample evidence to prove this theory. When considering the possibilities of where LRRK2 resides in regard to the nucleus, its large size makes it improbable that LRRK2 would reside in the nucleus. Also, it does not seem to have a nuclear localization sequence to reach the nucleus on its own, as a comparison was run on the LRRK2 sequence using the ExPASY Proteomics server to a consensus nuclear localization sequence resulting in no matches (no similarities) [70]. There is the possibility that a chaperone could escort it there. However, other studies have shown that LRRK2, through immunocytochemistry and subcellular fractionation, is a cytoplasmic protein providing further evidence that the protein is not within the nucleus.

The LRRK2 protein may be associated with the microtubule network

As a result of the slight co-localization seen in the R1441C mutant with the intermediate filaments, it was of interest to determine what would happen if the microtubules were depolymerized. Using colchicine -- which binds to tubulin thereby preventing microtubule polymerization --, after transfecting cells with the LRRK2 Rab constructs, microtubules were depolymerized to examine if there was a change in the intermediate filament structures. Treatment led to a complete depolymerization of the microtubules, and a collapse in the intermediate filament network. The LRRK2 Rab wild type and R1398L phenotypes did not show any significant changes (Figures 16A and B). When observing the R1441C mutant to see if its phenotype was affected however, the filamentous structures observed in one third of untreated transfected cells completely disappeared when microtubules were depolymerized (Figure 16C). The protein appeared as the wild type, "usual" morphology, punctate within the cytosol, showing slight co-localization with the depolymerized microtubules, providing further evidence that LRRK2 is associated with the microtubule network.

Microtubule depolymerization could lead to various affects within the cell, as this network is essential for cell resilience, especially in maintaining the cytoskeleton in association with the microfilaments and intermediate filaments. Vimentin is one of six types of intermediate filaments found within the cell. Therefore, LRRK2 could possibly associate with the other types of intermediate filaments in this cytoskeletal network. It should be noted however, that the vimentin filaments did not completely disappear upon the addition of colchicine, but collapsed from an outstretched network toward the cell nucleus. Therefore it would be expected that the other intermediate filament types would have the same effect after the addition of colchicine.

Dysfunction of the microtubule system is emerging as a contributing factor in a number of neurodegenerative diseases [71]. Other genes associated with PD have been suggested to work with or be affected by the microtubules [56, 72]. In a study by Alim et al [71], the influence of the neurotoxin 1-methyl-4-phenylpyridinium (MPP+) -- which kills dopamine neurons resulting in parkinsonian-like symptoms --, on microtubules was investigated [71]. This toxin has become a tool to study sporadic PD. The results showed that MPP+ affected microtubule dynamics *in vitro* as it reduced the average length and the number of microtubules nucleated from centrosomes. It should be noted however that this may not be the sole cause of death by MPP+.

It was proposed that a limited range of acceptable microtubule dynamic behaviours existed in neurons, outside of which microtubules could not function normally leading to cell death [73]. Among the microtubule-dependent functions, axonal transport could be a good candidate to explain how a cell could die following microtubule dysfunction. Another possibility is that the interference with the dynamics of axonal microtubules could drastically compromise synaptic functionality by, for instance, interfering with microtubule-associated proteins that regulate neurite length and growth. In a paper by MacLeod and colleagues, LRRK2 was shown to regulate neurite outgrowth [55], which was disrupted by mutations. This group also suggested that a LRRK2 target could be tau, a microtubule associated protein that is involved in axonal transport, which is associated with neurodegeneration. In LRRK2 associated PD, tau deposits have been found in some carriers of the R1441C mutation. Even though a direct connection between LRRK2 and tau has yet to be identified, it would be interesting to discover if there is a possible indirect relation between the two proteins.

The data presented in this paper along with other studies of LRRK2 suggest that somehow, LRRK2 is involved in the microtubule network, and disruptions, either through mutations, or neurotoxins, could lead to microtubule instability resulting in cell death as a final outcome of PD. The R1441C mutant unusual phenotype may help uncover proteins that work with LRRK2 to result in death if LRRK2 is not regulated properly.

The filamentous structures of the R1441C mutant may present an avenue to determine LRRK2 interactors.

The filamentous structures highlighted by the LRRK2 R1441C mutant in some cells, seem to be usually located around the nucleus. Therefore, proteins in a subregion just outside or within the nuclear envelope may associate with LRRK2. Mutations therefore, may compromise the nuclear envelope or structures associated with it such as the ER, microtubules, or cytoskeletal elements which could cause the death phenotype observed solely in neuronal cells.

This has led to the idea that LRRK2 is working with a neuronal protein that causes either over activation or deactivation of a cell process resulting in cell death. This also however could work in reverse, as other cell types may have a protein not present in neurons allowing proper regulation of the LRRK2 protein.

When observing the morphology of LRRK2 in CHO cells, namely the R1441C construct, there were filamentous structures around the nucleus. These perinuclear structures could associate with different structures in the cell. If considering the first idea mentioned in the above paragraph, that a specific neuronal protein is working with LRRK2, the torsin protein could be an interesting target. Torsin A is a protein located in

the lumen of the ER of neuronal cells which, if related to the results presented here, may be indirectly associated with these filamentous structures within the cytoplasm since it has a similar phenotype in this region albeit residing in the lumen of the nuclear envelope and associated ER.

Torsin A is a protein that is both highly expressed in dopamine neurons and is a component of Lewy bodies, where it closely associates with alpha-synuclein [74, 75]. Torsin A belongs to the functionally diverse AAA protein family (ATPases associated with cellular activities) that includes heat shock proteins (Hsp), proteases, and dynein [76]. It has been demonstrated to possess chaperone activity and can suppress intracellular protein aggregation *in vivo.* Dominant mutations in the *DYT1* gene encoding Torsin A cause early-onset torsion dystonia (EOTD), another movement disorder in which aberrant dopamine signaling has been suggested to play a role. Moreover, Torsin A was found recently to modulate cellular levels of the dopamine transporter (DAT). If therefore, this protein has a regulatory effect in the nigrostriatal pathway, and if LRRK2 causes it to become compromised, this in turn could lead to the PD symptoms and phenotype that result due to improper LRRK2 function resulting in neuronal cell death. This would not affect other cell types however, because of torsin's neuronal specificity.

When mentioning chaperone activity, LRRK2 was indeed shown to be stabilized by Heat Shock Protein 90 (Hsp 90) [77]. Hsp 90 contributes to the stability, activity, and translocation of protein kinases. If Torsin A also behaves in this manner, there is the possibility that it may interact with LRRK2 as a chaperone, aiding in stability.

Some interesting issues arose from this research, the most important being the cause of cell death when overexpressing LRRK2 in neuronal cells. The evidence

presented supports the proposal that LRRK2 overexpression led to neuronal cell degeneration.

To coincide with other research groups, mutations in the Rab domain of LRRK2 were shown to lead to a decreased rate of GTP hydrolysis. Disruption in hydrolysis could lead to a change in cellular morphology of LRRK2 as seen in the R1441C mutant. If LRRK2 is associated with the microtubule network, mutations within the LRRK2 Rab could result in a hyperactive kinase, which could lead to a destabilization in the microtubule network, and eventually, death seen through the Trypan Blue assay, but mainly observed in PD pathogenesis.

Identifying proteins that interact with LRRK2, the domains with which they interact, and especially, determining the substrate of the LRRK2 kinase domain could reveal answers to many questions that have been associated with LRRK2. The evidence presented here suggests that these proteins may, along with LRRK2, be involved in the microtubule network. Identifying the main role of the LRRK2 protein in cellular events can help discern the molecular mechanisms relating cell death to PD. This discovery could lead to possible therapeutic targets to help patients eventually recover from this debilitating disease.

REFERENCES

1. Paisan-Ruiz, C., et al., *Cloning of the gene containing mutations that cause PARK8-linked Parkinson's disease.* Neuron, 2004. **44**(4): p. 595-600.
2. Li, C. and M.F. Beal, *Leucine-rich repeat kinase 2: a new player with a familiar theme for Parkinson's disease pathogenesis.* Proc Natl Acad Sci U S A, 2005. **102**(46): p. 16535-6.
3. Zimprich, A., et al., *Mutations in LRRK2 cause autosomal-dominant parkinsonism with pleomorphic pathology.* Neuron, 2004. **44**(4): p. 601-7.
4. Marin, I., *The Parkinson disease gene LRRK2: evolutionary and structural insights.* Mol Biol Evol, 2006. **23**(12): p. 2423-33.
5. Tan, E.K., et al., *The LRRK2 Gly2385Arg variant is associated with Parkinson's disease: genetic and functional evidence.* Hum Genet, 2007. **120**(6): p. 857-63.
6. Hodaie, M., J.S. Neimat, and A.M. Lozano, *The dopaminergic nigrostriatal system and Parkinson's disease: molecular events in development, disease, and cell death, and new therapeutic strategies.* Neurosurgery, 2007. **60**(1): p. 17-28; discussion 28-30.
7. Benmoyal-Segal, L. and H. Soreq, *Gene-environment interactions in sporadic Parkinson's disease.* J Neurochem, 2006. **97**(6): p. 1740-55.
8. Wood-Kaczmar, A., S. Gandhi, and N.W. Wood, *Understanding the molecular causes of Parkinson's disease.* Trends Mol Med, 2006. **12**(11): p. 521-8.
9. Holtz, W.A., et al., *Oxidative stress-triggered unfolded protein response is upstream of intrinsic cell death evoked by parkinsonian mimetics.* J Neurochem, 2006. **99**(1): p. 54-69.
10. Ryu, E.J., et al., *Endoplasmic reticulum stress and the unfolded protein response in cellular models of Parkinson's disease.* J Neurosci, 2002. **22**(24): p. 10690-8.
11. Cookson, M.R., *The biochemistry of Parkinson's disease.* Annu Rev Biochem, 2005. **74**: p. 29-52.
12. Belin, A.C. and M. Westerlund, *Parkinson's disease: A genetic perspective.* FEBS J, 2008. **275**(7): p. 1377-83.
13. Kruger, R., et al., *Parkinson's disease: one biochemical pathway to fit all genes?* Trends Mol Med, 2002. **8**(5): p. 236-40.
14. Zabetian, C.P., et al., *LRRK2 G2019S in families with Parkinson disease who originated from Europe and the Middle East: evidence of two distinct founding events beginning two millennia ago.* Am J Hum Genet, 2006. **79**(4): p. 752-8.
15. Tan, E.K., et al., *The G2019S LRRK2 mutation is uncommon in an Asian cohort of Parkinson's disease patients.* Neurosci Lett, 2005. **384**(3): p. 327-9.
16. Mata, I.F., et al., *LRRK2 in Parkinson's disease: protein domains and functional insights.* Trends Neurosci, 2006. **29**(5): p. 286-93.
17. Haugarvoll, K., et al., *Lrrk2 R1441C parkinsonism is clinically similar to sporadic Parkinson disease.* Neurology, 2008. **70**(16 Pt 2): p. 1456-60.
18. Toft, M., et al., *LRRK2 mutations are not common in Alzheimer's disease.* Mech Ageing Dev, 2005. **126**(11): p. 1201-5.
19. Kay, D.M., et al., *Escaping Parkinson's disease: a neurologically healthy octogenarian with the LRRK2 G2019S mutation.* Mov Disord, 2005. **20**(8): p. 1077-8.

20. Ross, O.A. and M.J. Farrer, *Pathophysiology, pleiotrophy and paradigm shifts: genetic lessons from Parkinson's disease.* Biochem Soc Trans, 2005. **33**(Pt 4): p. 586-90.
21. Ridley, A.J., *Rho family proteins: coordinating cell responses.* Trends Cell Biol, 2001. **11**(12): p. 471-7.
22. White, L.R., et al., *MAPK-pathway activity, Lrrk2 G2019S, and Parkinson's disease.* J Neurosci Res, 2007. **85**(6): p. 1288-94.
23. Miklossy, J., et al., *LRRK2 expression in normal and pathologic human brain and in human cell lines.* J Neuropathol Exp Neurol, 2006. **65**(10): p. 953-63.
24. Galter, D., et al., *LRRK2 expression linked to dopamine-innervated areas.* Ann Neurol, 2006. **59**(4): p. 714-9.
25. Higashi, S., et al., *Localization of Parkinson's disease-associated LRRK2 in normal and pathological human brain.* Brain Res, 2007. **1155**: p. 208-19.
26. Melrose, H., et al., *Anatomical localization of leucine-rich repeat kinase 2 in mouse brain.* Neuroscience, 2006. **139**(3): p. 791-4.
27. Melrose, H.L., et al., *A comparative analysis of leucine-rich repeat kinase 2 (Lrrk2) expression in mouse brain and Lewy body disease.* Neuroscience, 2007. **147**(4): p. 1047-58.
28. Westerlund, M., et al., *Developmental regulation of leucine-rich repeat kinase 1 and 2 expression in the brain and other rodent and human organs: Implications for Parkinson's disease.* Neuroscience, 2008. **152**(2): p. 429-36.
29. Biskup, S., et al., *Dynamic and redundant regulation of LRRK2 and LRRK1 expression.* BMC Neurosci, 2007. **8**: p. 102.
30. Wang, D., et al., *Dispensable role of Drosophila ortholog of LRRK2 kinase activity in survival of dopaminergic neurons.* Mol Neurodegener, 2008. **3**: p. 3.
31. Zhu, X., et al., *LRRK2 protein is a component of Lewy bodies.* Ann Neurol, 2006. **60**(5): p. 617-8; author reply 618-9.
32. Giasson, B.I., et al., *Biochemical and pathological characterization of Lrrk2.* Ann Neurol, 2006. **59**(2): p. 315-22.
33. Gloeckner, C.J., et al., *The Parkinson disease causing LRRK2 mutation I2020T is associated with increased kinase activity.* Hum Mol Genet, 2006. **15**(2): p. 223-32.
34. Smith, W.W., et al., *Leucine-rich repeat kinase 2 (LRRK2) interacts with parkin, and mutant LRRK2 induces neuronal degeneration.* Proc Natl Acad Sci U S A, 2005. **102**(51): p. 18676-81.
35. Hatano, T., et al., *Leucine-rich repeat kinase 2 associates with lipid rafts.* Hum Mol Genet, 2007. **16**(6): p. 678-90.
36. Biskup, S., et al., *Localization of LRRK2 to membranous and vesicular structures in mammalian brain.* Ann Neurol, 2006. **60**(5): p. 557-69.
37. Gandhi, P.N., et al., *The Roc domain of leucine-rich repeat kinase 2 is sufficient for interaction with microtubules.* J Neurosci Res, 2008.
38. Chang, L. and M. Karin, *Mammalian MAP kinase signalling cascades.* Nature, 2001. **410**(6824): p. 37-40.
39. Greggio, E., et al., *Kinase activity is required for the toxic effects of mutant LRRK2/dardarin.* Neurobiol Dis, 2006. **23**(2): p. 329-41.

40. Li, X., et al., *Leucine-rich repeat kinase 2 (LRRK2)/PARK8 possesses GTPase activity that is altered in familial Parkinson's disease R1441C/G mutants.* J Neurochem, 2007. **103**(1): p. 238-47.
41. Smith, W.W., et al., *Kinase activity of mutant LRRK2 mediates neuronal toxicity.* Nat Neurosci, 2006. **9**(10): p. 1231-3.
42. West, A.B., et al., *Parkinson's disease-associated mutations in leucine-rich repeat kinase 2 augment kinase activity.* Proc Natl Acad Sci U S A, 2005. **102**(46): p. 16842-7.
43. Guo, L., W. Wang, and S.G. Chen, *Leucine-rich repeat kinase 2: relevance to Parkinson's disease.* Int J Biochem Cell Biol, 2006. **38**(9): p. 1469-75.
44. Wennerberg, K., K.L. Rossman, and C.J. Der, *The Ras superfamily at a glance.* J Cell Sci, 2005. **118**(Pt 5): p. 843-6.
45. Korr, D., et al., *LRRK1 protein kinase activity is stimulated upon binding of GTP to its Roc domain.* Cell Signal, 2006. **18**(6): p. 910-20.
46. Bosgraaf, L. and P.J. Van Haastert, *Roc, a Ras/GTPase domain in complex proteins.* Biochim Biophys Acta, 2003. **1643**(1-3): p. 5-10.
47. Taylor, J.P., et al., *Leucine-rich repeat kinase 1: a paralog of LRRK2 and a candidate gene for Parkinson's disease.* Neurogenetics, 2007. **8**(2): p. 95-102.
48. Paduch, M., F. Jelen, and J. Otlewski, *Structure of small G proteins and their regulators.* Acta Biochim Pol, 2001. **48**(4): p. 829-50.
49. Ali, B.R. and M.C. Seabra, *Targeting of Rab GTPases to cellular membranes.* Biochem Soc Trans, 2005. **33**(Pt 4): p. 652-6.
50. Pfeffer, S., *A model for Rab GTPase localization.* Biochem Soc Trans, 2005. **33**(Pt 4): p. 627-30.
51. Deng, J., et al., *Structure of the ROC domain from the Parkinson's disease-associated leucine-rich repeat kinase 2 reveals a dimeric GTPase.* Proc Natl Acad Sci U S A, 2008. **105**(5): p. 1499-504.
52. Ito, G., et al., *GTP binding is essential to the protein kinase activity of LRRK2, a causative gene product for familial Parkinson's disease.* Biochemistry, 2007. **46**(5): p. 1380-8.
53. Guo, L., et al., *The Parkinson's disease-associated protein, leucine-rich repeat kinase 2 (LRRK2), is an authentic GTPase that stimulates kinase activity.* Exp Cell Res, 2007. **313**(16): p. 3658-70.
54. Lewis, P.A., et al., *The R1441C mutation of LRRK2 disrupts GTP hydrolysis.* Biochem Biophys Res Commun, 2007. **357**(3): p. 668-71.
55. MacLeod, D., et al., *The familial Parkinsonism gene LRRK2 regulates neurite process morphology.* Neuron, 2006. **52**(4): p. 587-93.
56. Alim, M.A., et al., *Tubulin seeds alpha-synuclein fibril formation.* J Biol Chem, 2002. **277**(3): p. 2112-7.
57. Yang, F., Jiang, Q., Zhao, J., Ren, Y., Sutton, M. D., Feng, J., *Parkin stabilizes microtubules through strong binding mediated by three independent domains.* J Biol Chem, 2005. **280**: p. 17154-17162.
58. Jaleel, M., et al., *LRRK2 phosphorylates moesin at threonine-558: characterization of how Parkinson's disease mutants affect kinase activity.* Biochem J, 2007. **405**(2): p. 307-17.

59. Bialik, S., Bresnick, A. R., Kimchi., A., *DAP-kinase-mediated morphological changes are localization dependent and involve myosin-II phosphorylation.* Cell Death Differ, 2004. **11**: p. 631-644.
60. Leonard, M., et al., *Robust colorimetric assays for dynamin's basal and stimulated GTPase activities.* Methods Enzymol, 2005. **404**: p. 490-503.
61. Brewton, L.S., L. Haddad, and E.C. Azmitia, *Colchicine-induced cytoskeletal collapse and apoptosis in N-18 neuroblastoma cultures is rapidly reversed by applied S-100beta.* Brain Res, 2001. **912**(1): p. 9-16.
62. Goldman, R.D., et al., *The function of intermediate filaments in cell shape and cytoskeletal integrity.* J Cell Biol, 1996. **134**(4): p. 971-83.
63. Sorci, G., et al., *Association of S100B with intermediate filaments and microtubules in glial cells.* Biochim Biophys Acta, 1998. **1448**(2): p. 277-89.
64. Greggio, E., et al., *The Parkinson's disease associated Leucine rich repeat kinase 2 (LRRK2) is a dimer that undergoes intra-molecular autophosphorylation.* J Biol Chem, 2008.
65. Wittmann, J.G. and M.G. Rudolph, *Crystal structure of Rab9 complexed to GDP reveals a dimer with an active conformation of switch II.* FEBS Lett, 2004. **568**(1-3): p. 23-9.
66. Pasqualato, S., et al., *The structural GDP/GTP cycle of Rab11 reveals a novel interface involved in the dynamics of recycling endosomes.* J Biol Chem, 2004. **279**(12): p. 11480-8.
67. Avruch, J., et al., *Ras activation of the Raf kinase: tyrosine kinase recruitment of the MAP kinase cascade.* Recent Prog Horm Res, 2001. **56**: p. 127-55.
68. Zhang, B. and Y. Zheng, *Negative regulation of Rho family GTPases Cdc42 and Rac2 by homodimer formation.* J Biol Chem, 1998. **273**(40): p. 25728-33.
69. Pelech, S., *Dimerization in protein kinase signaling.* J Biol, 2006. **5**(5): p. 12.
70. De Castro E., S.C.J.A., Gattiker A., Bulliard V.,Langendijk-Genevaux P.S., Gasteiger E., Bairoch A., Hulo N., *ScanProsite: detection of PROSITE signature matches andProRule-associated functional and structural residues in proteins.* Nucleic Acids Res., 2006. **34 (Web server issue)**.
71. Cappelletti, G., T. Surrey, and R. Maci, *The parkinsonism producing neurotoxin MPP+ affects microtubule dynamics by acting as a destabilising factor.* FEBS Lett, 2005. **579**(21): p. 4781-6.
72. Kitada, T., et al., *Mutations in the parkin gene cause autosomal recessive juvenile parkinsonism.* Nature, 1998. **392**(6676): p. 605-8.
73. Feinstein, S.C. and L. Wilson, *Inability of tau to properly regulate neuronal microtubule dynamics: a loss-of-function mechanism by which tau might mediate neuronal cell death.* Biochim Biophys Acta, 2005. **1739**(2-3): p. 268-79.
74. Shashidharan, P., et al., *TorsinA accumulation in Lewy bodies in sporadic Parkinson's disease.* Brain Res, 2000. **877**(2): p. 379-81.
75. Sharma, N., et al., *A close association of torsinA and alpha-synuclein in Lewy bodies: a fluorescence resonance energy transfer study.* Am J Pathol, 2001. **159**(1): p. 339-44.
76. Neuwald, A.F., et al., *AAA+: A class of chaperone-like ATPases associated with the assembly, operation, and disassembly of protein complexes.* Genome Res, 1999. **9**(1): p. 27-43.

77. Wang, L., et al., *The chaperone activity of heat shock protein 90 is critical for maintaining the stability of leucine-rich repeat kinase 2.* J Neurosci, 2008. **28**(13): p. 3384-91.